SEMMELWEIS EGYETEM

DOKTORI ISKOLA

Ph.D. értekezések

3058.

PEDRO HENRIQUE LEROY VIANA

Kórélettan és transzlációs medicina
című program

Programvezető: Dr. Benyó Zoltán, egyetemi tanár

Témavezető: Dr. Hamar Péter, egyetemi tanár

ENHANCEMENT OF MODULATED ELECTRO-HYPERTHERMIA EFFECTS BY HEAT SHOCK FACTOR 1 INHIBITION AND RE-SENSITIZATION OF CANCER CELLS TO ANTIPROGESTINS IN A TRIPLE-NEGATIVE BREAST CANCER MODEL

PhD thesis

Pedro Henrique Leroy Viana

Semmelweis University Doctoral School

Theoretical and Translational Medicine Division

Supervisor: Péter Hamar, MD, DSc

Official reviewers: János Barna, PhD
Ambrus Gángó, MD, PhD

Head of the Complex Examination Committee: György Losonczy, MD, DSc

Members of the Complex Examination Committee: Andrea Székely, MD, DSc
Ákos Jobbágy, DSc

Budapest
2024

Contents

List of Abbreviations

cHT – Conventional Hyperthermia

CRISPR/Cas9 – Clustered Regularly Interspaced Palindromic Repeats

DAB – 3, 3'-diaminobenzidine

DE – Differential Expression

DMEM – Dulbecco's Modified Eagle Medium

DNA – Deoxyribonucleic Acid

ECM – Extracellular Matrix

EMT – Epithelial-Mesenchymal Transition

EV – Empty Vector

FACS – Fluorescence-Activated Cell Sorting

FBS – Fetal Bovine Serum

FC – Fold Change

GFP – Green Fluorescent Protein

gRNA – Guide RNA

H&E – Hematoxylin and Eosin

HCC – Hepatocellular Carcinoma

HER2 – Human Epidermal Growth Factor Receptor 2

HSE – Heat Shock Elements

HSF1 – Heat Shock Factor 1

HSP – Heat Shock Proteins

HSR – Heat Shock Response

IC_{50} – Half Maximum Inhibitory Concentration

IHC – Immunohistochemistry

ICM – Intracellular Matrix

KO – Knockdown

MEF – Mouse Embryonic Fibroblasts

mEHT – Modulated Electro-Hyperthermia

MIF – Mifepristone

mRNA – Messenger Ribonucleic Acid

MS – Mass Spectrometry

NGS – Next-Generation Sequencing

ns – Not Significant

OSCC – Oral Squamous Cell Carcinoma

p-TEFb – Positive Transcription Elongation Factor b

PBS – Phosphate-Buffered Saline

PCR – Polymerase Chain Reaction

PGR – Progesterone Receptor

PRA – Progesterone Receptor Isoform A

PRE – Progesterone Response Elements

RF – Radiofrequency

rMA – Relative Masked Area

RNA – Ribonucleic Acid

ROS – Reactive Oxygen Species

SD – Standard Deviation

siRNA – Small Interfering RNA

SPRM – Selective Progesterone Receptor Modulator

TDR – Tumor Destruction Ratio

TNBC – Triple-Negative Breast Cancer

UPA – Ulipristal Acetate

VEGF – Vascular Endothelial Growth Factor

Veh – Vehicle

WT – Wild type

1. Introduction

1.1. Triple-Negative Breast Cancer

Cancer is a major public health problem and the leading cause of death worldwide, accounting for nearly 10 million deaths in 2020 (1). Female breast cancer is the most diagnosed cancer type and has surpassed lung cancer as the leading cause of global cancer incidence in 2020, with an estimated 2.3 million new cases, representing 11.7% of all cancer cases and 684,996 of cancer deaths (1).

Among all breast cancer types, triple-negative breast cancer (TNBC) is the most aggressive clinical subtype, characterized by its metastatic patterns and resulting in a poor prognosis (2). TNBC refers to the subset of breast cancers lacking estrogen-, progesterone-, and human epidermal growth factor 2 receptors (HER2) (3, 4). TNBC represents 15-20% of all breast cancer patients and tends to have higher incidence among premenopausal young women under 40 years of age (5). It is characterized by distinct biological features, unfavorable course, and high histological grade (6, 7). In comparison to other subtypes of breast cancer, TNBC patients have shorter survival time, with a mortality rate of 40% within the first 5 years after diagnosis (8), mostly because TNBC is highly invasive and likely 46% of TNBC patients will experience distant metastasis (9). Due to the absence of receptor expression, TNBC is not sensitive to endocrine treatment and targeted therapies (10, 11). Although many efforts have been made to develop treatment options for patients with TNBC (4, 12), still the few available treatments are surgery, chemotherapy, and/or radiotherapy (5), all with poor outcome. Therefore, the development of new treatment strategies is urgently needed.

1.2. Heat Shock Response

The heat shock response (HSR) is a fundamental cellular mechanism that plays a critical role in maintaining proteostasis and cellular homeostasis under stress conditions (13). The heat shock factor 1 (HSF1) is the master regulator of the HSR in eukaryotes (14, 15). HSF1 is an ubiquitously expressed

transcription factor that regulates the expression of heat shock protein (HSP) genes in response to cellular stress (16). To avoid cellular damage and protein degradation caused by a wide range of environmental stressors, organisms respond by inducing HSPs, which refold damaged proteins, consequently preserving proteostasis (17). The process unfolds as follows: upon heat shock (or other forms of cellular stress), HSF1 is phosphorylated, trimerizes, and translocates into the nucleus, where it induces chaperone gene expression by binding to DNA sequence motifs known as heat shock elements (HSEs) (18), the promoter regions of HSPs. Consequently, transcription of HSP genes is induced (19). HSPs in turn interact and regulate HSF1 transcriptional activity by direct binding, creating a negative feedback mechanism for controlling the HSR (20). Cell survival is achieved through the activation of anti-apoptotic proteins and the inhibition of pro-apoptotic proteins, a phenomenon known as thermotolerance, which enables cancer cells to withstand the effects of heat (18). **Figure 1** illustrates the HFS1 activation. Hence, the role of HSPs is to regulate protein (re)folding, transport, translocation, and assembly under stress conditions in many normal cellular processes (21). Therefore, upregulation of HSPs increases cell survival and stress tolerance (22), not only in healthy cells under any kind of stress but also in cancer cells in which elevated expression of different members of the HSP family has been reported (23, 24).

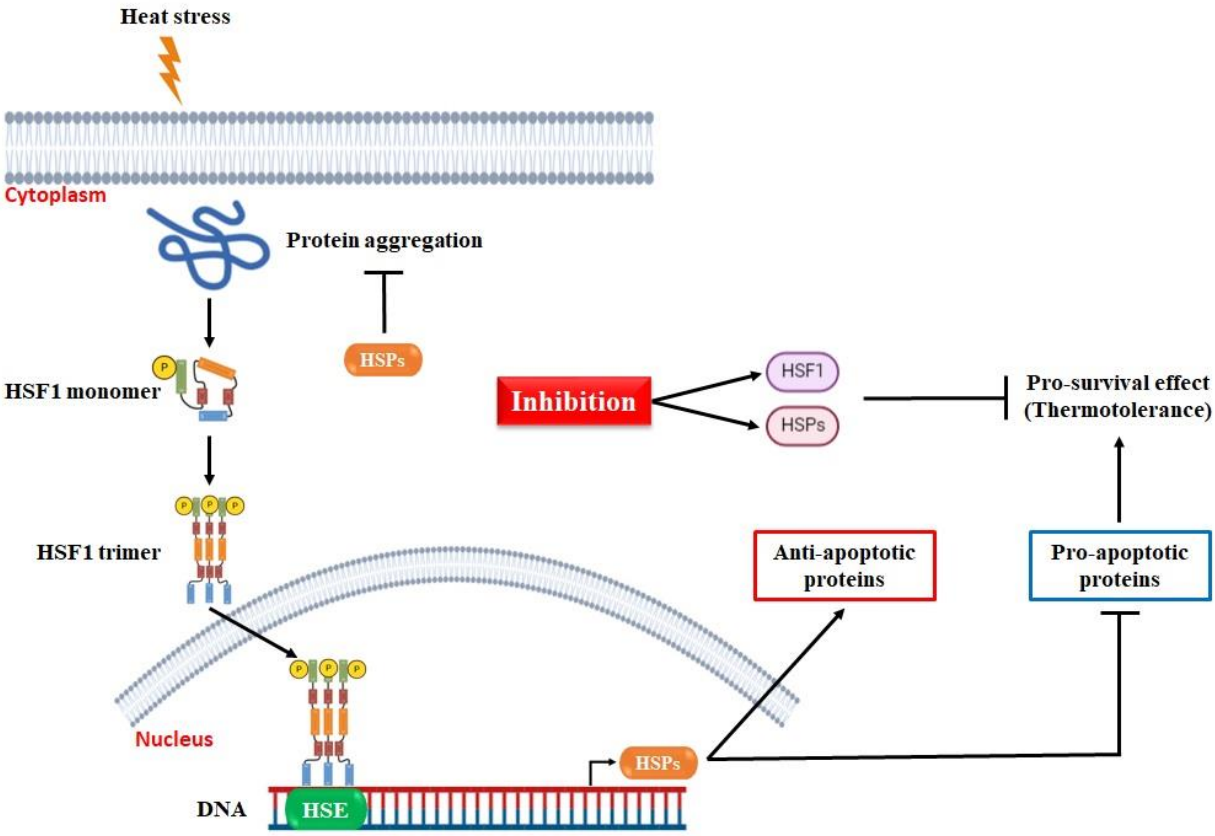

Figure 1. Heat-induced thermotolerance. Heat stress leads to aggregation of HSF1 monomer into DNA binding homotrimer. This HSF1 trimer translocates to the nucleus where it binds to heat shock elements (HSE) in the promoters of HSP genes, inducing the transcription of heat shock proteins (HSPs). HSPs (chaperones) protect proteins from aggregation and activate anti-apoptotic proteins and inhibit pro-apoptotic proteins, leading to thermotolerance. Therefore, heat-induced thermotolerance protects cells from hyperthermia-induced apoptosis. HSF1: heat shock factor 1; HSE: heat shock elements; HSP: heat shock protein; DNA: deoxyribonucleic acid; P: phosphate. Based on Ahmed *et al.* (18). Published by Viana *et al.* (25). Created with biorender.com.

1.2.1. The Role of Heat Shock Response and HSF1 in Cancer

The heat shock response (HSR) plays a crucial role in cancer. Once dysregulated, the HSR contributes to the survival and growth of cancer cells (26). In the malignant state, a wide variety of stressful conditions, such as hypoxia, acidity, and low glucose levels, arises from the tumor microenvironment (27). In all these stress conditions, the cell's proteostasis network, which is responsible for the balance of protein synthesis, folding, and degradation, can be overwhelmed (28). Therefore, cancer cells have constantly

activated HSR and elevated proteasome activities due to the high levels of constitutively misfolded proteins. HSF1, as the master regulator of the HSR, permits cancer cells to cope with these diverse malignancy-associated stressors. In doing so, malignant tumors reprogram their metabolism, physiology, and protein homeostasis, enabling oncogenesis (29). This enhanced cytoprotective response enables cancer cells to withstand cellular stress, proliferate, and develop resistance to conventional cancer therapies (30). The ultimate result is the facilitated cellular adaptation to the malignant lifestyle (31). Additionally, the HSR has been implicated in cancer cell invasion, angiogenesis, and immune evasion (32). In cancer, HSF1 controls many genes, such as cell cycle and apoptosis regulators, that contribute to the malignant phenotype and support cancer growth (33), including genes involved in cell-cycle regulation, signaling, metabolism, adhesion and translation (34). While HSF1 mutations are uncommon in different cancer types, frequent copy number alterations, particularly amplifications, are prevalent (35). Indeed, many human cancer types and cancer cell lines express HSF1 constitutively at elevated levels (17, 36, 37), including hepatocellular carcinoma (HCC) (38, 39), breast cancer (29), endometrial carcinoma (40), and oral squamous cell carcinoma (OSCC) (41).

In cancer cells, HSF1 is often constitutively activated, leading to abnormal upregulation of HSPs, which confers a selective advantage to malignant cells by promoting cell survival, inhibiting apoptosis, and aiding in the development of aggressive phenotypes (32). The oncogenic potential of HSF1 was initially revealed by HSF1-knockdown mouse models (31). Indeed, HSF1 knockdown investigations have shed light on the crucial role of this protein in cancer growth, and the use of siRNA or genetic mutation to silence HSF1 has demonstrated a substantial reduction in tumorigenicity across multiple cancer types (42). On the other hand, the overexpression and hyperactivation of HSF1 have been linked to poor prognosis and drug resistance in several cancer types, making it an attractive target for cancer therapy (43).

Although much less is known about the molecular mechanisms by which HSF1 regulates cell proliferation and survival in cancer cells, elevated expression levels of different members of the stress-inducible HSP family have

been reported in a wide range of cancer types, indicating a crucial role of HSPs in tumor development (23, 44). Indeed, overexpression of HSPs have received considerable attention as prognostic biomarkers in terms of survival and response to therapy in cancer (45). The elevated levels of HSPs provide cancer cells a survival advantage by promoting protein folding, stabilizing oncogenic proteins, and assisting the proper functioning of cellular processes under stress conditions (26). The hypoxic and nutrient-deprived tumor microenvironment induces proteotoxic stress and leads to HSPs upregulation as a cellular defense mechanism against misfolded proteins and aggregation (46, 47). Among the HSP-family members, the most extensively studied ones with active roles in cancer include HSP27, HSP70, and HSP90 (46). These HSPs exhibit slight functional variations and are commonly classified based on their molecular weight.

1.2.2. HSP70

HSP70 has a critical role in protein folding, protein homeostasis, and promoting cell survival (48). HSP70 is primarily expressed intracellularly in cancer cells (49), where it promotes survival, proliferation, invasiveness, and resistance of malignant cells. However, when shed or released extracellularly, HSP70 acts as a damage-associated molecular pattern (DAMP) that can contribute to antitumor immunity and increased cell damage (50, 51). Within cancer cells, HSP70 triggers mitotic signals, inhibits apoptosis, and suppresses oncogene-induced senescence (52). Overexpression of HSP70 is associated with resistance to chemotherapy and poor prognosis for a wide range of cancer types (51), such as lung, breast, colon, liver, prostate, esophagus, and cervix (53, 54). Moreover, the upregulated HSP70 levels could potentially work as a predictive factor for both cancer diagnosis and treatment response (52). Likewise, downregulation of HSP70 expression in preclinical setting inhibits cancer growth and significantly promotes apoptosis, consequently increasing malignant tumor's susceptibility to chemotherapy and radiotherapy (55).

1.3. Hyperthermia

Hyperthermia is a therapeutic approach that involves raising the temperature of a part of or the entire body to treat various medical conditions. In the context of cancer therapy, hyperthermia involves heating the cancerous area and can exploit the differential heat sensitivity between tumor tissue and normal, healthy tissue to enhance the effectiveness of treatments like chemotherapy and radiotherapy (56). Szasz *et al.* define oncological hyperthermia as "a method for killing malignant cells by controlled thermal effects, and has the potential to sensitize to complementary therapies while avoiding the destruction of healthy cells" (57). In fact, hyperthermia has been reported to be clinically relevant adjuvant therapy for cancer treatment (58). Many studies have demonstrated the increased drug exposure to cancer via the circulation by adding heat treatment, and hence increasing cytotoxicity of chemotherapeutic agents (59-62). However, hyperthermia as a cancer treatment modality has been reported to be controversial (63).

1.3.1. Hyperthermia in Oncology

The controversy surrounding hyperthermia therapy is due to challenges in achieving deep heat penetration and precise targeting. These challenges can lead to insufficient selective elimination of malignant cells and increased toxicity to healthy tissues (64). The ultimate result is an extensive macromolecular change that affects functions not only in tumor tissues but also in all adjacent cellular compartments, particularly when temperatures exceed 43°C (65). Additionally, an increase in temperature can boost blood flow and nutrient delivery, which potentially facilitates cancer progression and may aid metastasis development (66). Nonetheless, the most relevant complication associated with the use of hyperthermia in cancer treatment is the induction of heat stress response in cells (67, 68). This phenomenon, known as thermotolerance, is a cellular defense mechanism that reduces susceptibility to heat-induced damage (23). The mechanism of thermotolerance is attributed to HSP production, and hampers the effects of hyperthermia (27). This acquisition of thermotolerance enhances cancer cell growth by preventing apoptotic cell

death (18) via elevation of HSF1 (29) and HSPs (45), and reduces the hyperthermia effects in clinical treatment. Therefore, targeting HSF1 to inhibit the HSR might enhance the effectiveness of hyperthermia-based cancer treatments by increasing the sensitivity of cancer cells to heat-induced therapies.

1.3.2. Inhibition of Heat Shock Response Through HSF1

HSF1 is considered as one of the main determinants of oncogenesis, and ablation experiments have shed lights to the role of HSF1 in cancer development. *In vitro* HSF1 knockdown resulted in impairment of growth, survival, invasion, migration and epithelial-mesenchymal transition (EMT) of cancer cell lines, including pancreatic cancer (69, 70), multiple myeloma (71), hepatocellular carcinoma (HCC) (38), colorectal carcinoma (72), and melanoma (73). In turn, HSF1 knockout mouse models are proved to be remarkably resistant to a number of oncogenes (31, 74-76). Recently, it has been postulated that breast cancer tumors in HSF1 knockout mice, although viable, grow much slower than control tumors, suggesting that HSF1 plays a central role in cancer growth (77). Indeed, a chemically-induced carcinogenesis model revealed that $HSF1^{-/-}$ mice developed fewer tumors, presented lower tumor load (total amount of cancer in the body), and longer survival, while mice-bearing functional HSF1 developed larger tumors and had shorter survival (31). Moreover, HSF1 knockdown induces apoptosis (78), inhibits cell proliferation, and arrests cell cycle at G1 phase (72, 79) in cancer cells.

1.3.3. HSF1 Inhibition and Hyperthermia

HSF1 knockdown had been shown to enhance hyperthermic-chemotherapy in cervical cancer (80), and to reduce proliferation and tumor size in skin (31, 81), liver (78), ovarian (34), pancreatic (70), and breast (82, 83) cancers. Indeed, Rossi *et al.* reported that HSF1 knockdown led to increased sensitivity of HeLa cells to thermochemotherapy, resulting in upregulation of apoptosis (80). Also, the knockdown of HSF1 was associated with autophagy inhibition which increases drug sensitivity to chemotherapeutic treatment in

breast cancer cells (84). Interestingly, the knockdown of HSF1 seems to enhance cancer cell sensitivity to hyperthermia but does not have a direct influence on chemotherapy. Cancer cells' sensitivity to thermochemotherapy with or without HSF1 silencing was similar regarding cell destruction (81). In addition, the gene therapy designed to target HSF1 helped to escape thermotolerance in cancer cells (85-87). McMillan *et al.* have demonstrated that HSF1 inactivation abolished thermotolerance in mouse embryonic fibroblasts (MEF) treated with hyperthermia, and inhibited the upregulation of HSPs, such as HSP70 (88). Likewise, Wang and colleagues have demonstrated that functional silencing of HSF1 strongly reduced the HSP70 levels and inhibited thermotolerance in breast cancer cells, suggesting that cancer cells lacking HSP70 expression are sensitive to hyperthermia, and those overexpressing HSP70 may be thermotolerant (85). Moreover, HSF1 depletion by small interfering RNA (siRNA) resulted in reduction of the constitutively high expression of HSP90 and HSP70, in a breast cancer model (82). These findings suggest that hyperthermia in combination with the inhibition of the heat shock response might be exploited for treating cancer patients.

1.3.4. Modulated Electro-Hyperthermia

Modulated electro-hyperthermia (mEHT) is a promising adjuvant therapy form (89, 90). mEHT is a non-invasive cancer therapy applying a modulated electromagnetic field to the malignant tumor, inducing tumor cell damage by temperature dependent- and independent-mechanisms. A 13.56 MHz radiofrequency (RF) current is applied using capacitive coupling between two electrodes strategically arranged around the tumor (91, 92) (**Figure 2A**). The energy of the RF current is selectively absorbed by tumor tissues due to several mechanisms reviewed before (93), including cancer tissue metabolism, ion composition and the electromagnetic properties of lipid rafts (94). The electromagnetic field induces a +2.5 °C heating of the malignant tumor compared to its surrounding in preclinical setting (90). The +2.5 °C temperature difference, significantly widens the narrow therapeutic window (ΔT: ca 1 °C

only) achievable with conventional hyperthermia. The ultimate result is the minimal damage in surrounding normal tissues during mEHT treatments (95).

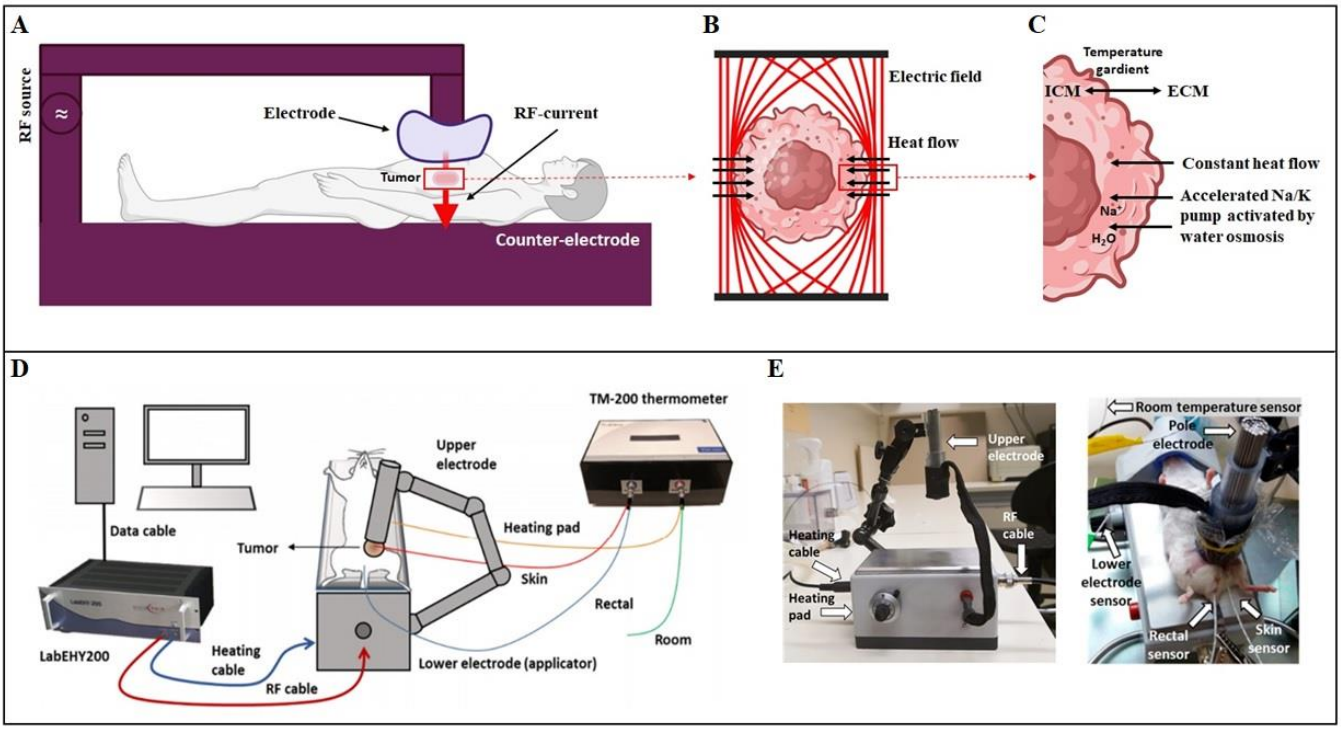

Figure 2. Schematic illustration of modulated electro-hyperthermia (mEHT) treatment in human patients and mice. The unidirectional electric field (depicted by the red arrow) traverses the patient's body, flowing in a controlled manner from the electrode to the counter-electrode **(A)**. This directional flow enables precise energy delivery to malignancies, particularly along cell membranes, exploiting the tendency of the electric field to follow paths of higher conductivity, such as malignant tissues. Consequently, this process induces localized heating **(B)**. Among subsequent biochemical reactions are alterations in membrane permeability, which are initiated by the heat stress in the cell membrane of malignant cells. The resulting temperature gradient between extracellular and intracellular matrices induces changes in membrane potential, triggering a series of events that includes heat transfer across the membrane, elevated intracellular sodium concentration, potassium efflux, and water osmosis **(C)**. The combined effects act synergistically and drive the induction of apoptosis. Based on Szasz *et. al* (64). Created with biorender.com **D)** Illustration of the mEHT treatment setup LabEHY200 designed for *in vivo* experiments involving mice, reproduced from Schvarcz *et. al* (89). **E)** mEHT *in vivo* treatment setup, reproduced from Danics *et. al* (90). RF: radiofrequency, ICM: intracellular matrix, ECM: extracellular matrix, Na: sodium, K: potassium. Published by Viana *et al.* (25).

1.3.5. Conventional Hyperthermia *vs* mEHT

The mEHT technique, which has been successfully applied in the clinics for over 30 years (95), differs from conventional hyperthermia methods, such

as non-modulated capacitive hyperthermia, in that mEHT creates a non-homogenous heating by increasing the temperature gradient between the intracellular/extracellular environment through the cell membranes in malignant tissues (96) (**Figure 2B**). This alteration in temperature gradient affects membrane processes, which favors signaling pathways that induce extrinsic apoptosis (95, 97) rather than thermal necrosis (98) (**Figure 2C**). The temperature dependent cytotoxicity targeting cancers is thus enhanced by a synergy between the heat and the electromagnetic field (99-103).

The fundamental concept behind mEHT was the rejection of the central reliance on temperature as the primary factor. Instead, the technology focused on the core elements of power absorption, extracellular heating, and modulation, which were not dependent on temperature (104). In fact, the modulation is able to induce non-thermal effects which enhance the cell-killing thermal effects, compared to conventional capacitive coupled hyperthermia (101, 105). Therefore, the resulting electromagnetic field generates irreversible cell stress (106). Moreover, mEHT has overcome the most problematic point of hyperthermia devices. According to Roussakow, the utilization of a 'skin sensor' in mEHT eliminates the requirement for thermometry traditionally employed in conventional hyperthermia techniques (104). The mEHT electrodes induce heating only surrounding the “zone of interest”, which increases selectivity of energy deposition in tumor tissues (104). In this regard, according to Lee *et al.*, mEHT is a promising technique that can achieve selective and effective targeting of the cancer tissue (63).

Previous *in vitro* and *in vivo* studies have demonstrated that mEHT is more effective than traditional hyperthermia (water-bath, infrared, or RF-hyperthermia) at the same temperature (105) due to the potentiating effects of the electromagnetic field (non-temperature dependent effects) and the greater temperature difference. **Figure 2D, E** illustrate the mouse setup for *in vivo* studies. Moreover, mEHT has been shown to enhance cell-killing effects by increasing drug uptake in cancer cells (107). In the clinical setting, mEHT has been demonstrated to induce significant enhancements, including increased

disease-free survival and improved quality of life, in patients with breast- (108), cervical- (109), ovarian- (110), rectal- (111), and pancreatic cancers (112-114).

1.3.6. The Mechanisms of Cancer Cell-Killing by mEHT

The mechanisms underlying mEHT involve a combination of thermal and non-thermal effects (**Figure 3**). The synergism between thermal and non-thermal effects triggers the excitation of specialized cell membrane regions, such as lipid rafts, ultimately resulting in activation of apoptotic pathways (97). The thermal effects are achieved by selectively heating tumor tissues through the absorption of electromagnetic waves by cancer cells, which leads to increased cellular temperature (103). These effects are, therefore, direct consequences of temperature elevation (temperature-dependent) through energy absorption. When exposed to elevated temperatures, cells undergo several changes that influence the progression of cell cycle (115). Application of mEHT induces irreversible cellular stress, resulting in the arrest of the cancer cell cycle and caspase-dependent programmed cell death (116, 117). The temperature elevation increases blood flow and perfusion through the target tissues, which potentially improve the efficacy of chemotherapy (118). Hyperthermia can also lead to protein denaturation due to the disruption of weak bonds and interactions with the protein's structure, causing it to unfold or lose its native conformation (119). This is the key event in the disruption of cellular homeostasis (18), and can be avoided by chaperone proteins, such as HSPs, that are able to prevent protein aggregation (120). Furthermore, in combination with chemotherapy and radiotherapy, mEHT has shown potential in overcoming hypoxia-related resistance (111, 121) and downregulating hypoxia-related target genes (120). Finally, the rise in temperature can induce localized acidosis through elevated metabolic activity and reduced oxygen availability (122). This harsh environment can ultimately lead to the destruction of the 'starving' malignant tumor (116).

On the another hand, mEHT also triggers non-thermal effects that occur when the system undergoes changes in its properties under the influence of an alternating electromagnetic field, which cannot be achieved solely through

heating (123), contributing to its anti-cancer properties. The non-thermal effects are primarily frequency-dependent and arise from the interaction between the biological substance and the RF-current rather than the heating process itself (124). Indeed, the high-frequency electric fields used in mEHT induce alterations in the electric potential across the cancer cell membranes, resulting in the formation of transient nanopores (125). These interactions subsequently engage the apoptotic signaling pathways (95). This phenomenon also known as electroporation can enhance the uptake of certain molecules and drugs, potentially increasing the treatment effectiveness (126). Furthermore, the conductivity and the dielectric constant in malignant tissues are higher compared to normal tissues (127). This leads to increased energy absorption by cancers compared to the surrounding healthy tissue, raising the extracellular temperature of cancer cells and ultimately causing damage (125). Through the electromagnetic field, mEHT is also able to induce direct DNA damage in cancer cells by several mechanisms, including the generation of reactive oxygen species (ROS) and the disruption of DNA repair pathways, which leads to genomic instability and cell death (120, 128). Moreover, previous study has confirmed that the electromagnetic field might inhibit or prevent new blood vessel formation through the vascular endothelial growth factor (VEGF) production in breast cancer cells (129), probably via disruption of bioelectric signals that impede the formation of new blood vessels. Finally, mEHT has been proposed to induce abscopal phenomena, leading to simultaneous growth inhibition of malignant tumors located at a distance from the site of treatment (130). By triggering an immune response reaction, mEHT enables the body to systematically recognize and attack cancer cells, shifting the balance towards cancer suppression (131). This is achieved through the induction of immunogenic cell death and modification of tumor microenvironment (97), leading to activation and recruitment of immune cells, such as dendritic (132), cytotoxic T (130), and natural killer cells (133). Additionally, mEHT may synergistically work with immune checkpoints inhibitors, which reinforce the immune response against cancer cells (134). The immune action of checkpoint inhibitors results in abscopal effect in clinical practice (135, 136).

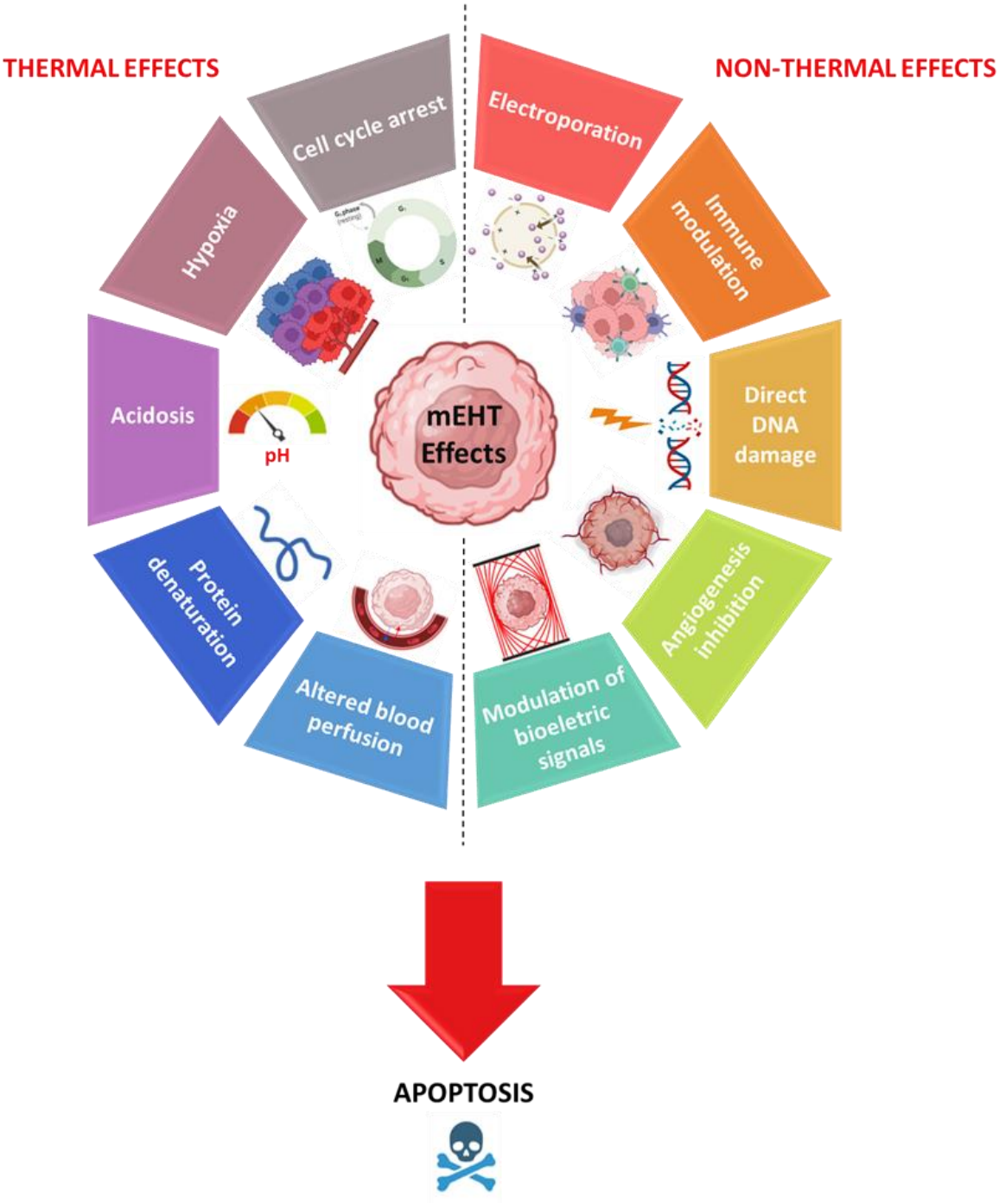

Figure 3. The figure highlights the intricate interplay between thermal and non-thermal influences induced by mEHT in cancer cells. Thermal effects encompass cell cycle arrest, hypoxia, acidosis, protein denaturation, and altered blood perfusion. Non-thermal effects include electroporation, immune modulation, direct DNA damage, angiogenesis inhibition, and modulation of bioelectric signals. These combined impacts emphasize the potential of mEHT as a comprehensive approach in cancer therapy. Based on (66, 111, 116, 118-120, 125, 127, 129, 131). Published by Viana *et al.* (25). Created with biorender.com.

1.3.7. mEHT and HSR induction

As mentioned before, when exposed to heat shock, cells produce chaperone proteins (heat shock proteins, HSPs) that protect them from the negative effects of heat. Same phenomena is observed in cancer cells, resulting in development of treatment resistance and the promotion of malignant processes including uncontrolled growth, reduced tumor suppression, enhanced cell survival, and the acquisition of powerful capacities for angiogenesis and metastasis (26). As a variation method of hyperthermia, mEHT can induce heat shock response and subsequent HSP upregulation in treated cancers. Indeed, the heat map on gene expression revealed significant induction of members of the heat shock protein family, such as HSP70 and HSP90, after mEHT treatment in a human colorectal adenocarcinoma xenografts (137). Multiplex data (Next Generation Sequencing – NGS, and NanoString), and qPCR confirmed the upregulation of HSP70 isoforms after mEHT treatments (89). Corroborating the upregulation in mRNA levels, HSPs were also upregulated at the protein level by immunohistochemistry (138) or Mass Spectrometry (MS).

The upregulation of HSP70 was also observed in a triple-negative breast cancer (TNBC) isografts treated with mEHT (89, 90). Moreover, mEHT increased more than 10-fold the extracellular HSP70 release 48 hours after treatment compared to conventional capacitive coupling hyperthermia and water bath (105). In another study, mEHT induced massive HSP70 expression not only intracellularly but also membrane-bound and extracellular HSP70 was stimulated, which can be linked to enhancement of anti-cancer immunity (139). In fact, Kuo *et al.* suggested that combined mEHT therapy with curcumin and resveratrol synergistically increased the immune response and HSP70 release, hence augmenting the anti-cancer efficacy in CT26 cells (140). mEHT is also able to provoke HSP70 upregulation in murine colon carcinoma models (106, 117, 132), pancreatic adenocarcinoma (141), and melanoma xenograft (133).

1.4. Inhibitors of the HSR

The activation of the Heat Shock Response (HSR) protects cancer cells from damage induced by heat, radiation, or chemotherapy, thereby reducing the efficacy of anticancer treatments (51). Indeed, overexpression of heat shock proteins has been identified as a survival mechanism in cancer, enabling them to resist therapeutic interventions (45). Suppressing this defense mechanism has the potential to enhance the sensitivity of cancer cells to hyperthermia and other anticancer therapies.

1.4.1. Natural and Synthetic HSF1 Inhibitors

Besides the studies that have demonstrated successful repression of cancer growth by depletion of the HSF1 gene, a number of attempts at developing small molecule inhibitors to reduce HSF1 expression have been reported (142) (**Figure 4**), but most of them are still in preclinical phase (43). In spite of the successful inhibition of HSF1 observed in both *in vitro* experiments and animal models, each inhibitor currently available for clinical use has its own set of limitations (143). Unfortunately, for many of these compounds, the exact mechanism of action and drug specificity remains unknown (43). Another bias comes from the fact that HSF1 carries restrictions as a target for drug development due to: the absence of a clearly identifiable binding site for small molecule inhibitors, the intricate nature of its activation process, and its susceptibility to numerous posttranslational modifications in response to different types and levels of proteotoxic stress (35). Nevertheless, targeting HSF1 for cancer therapy might be a promising modality in cancer treatment.

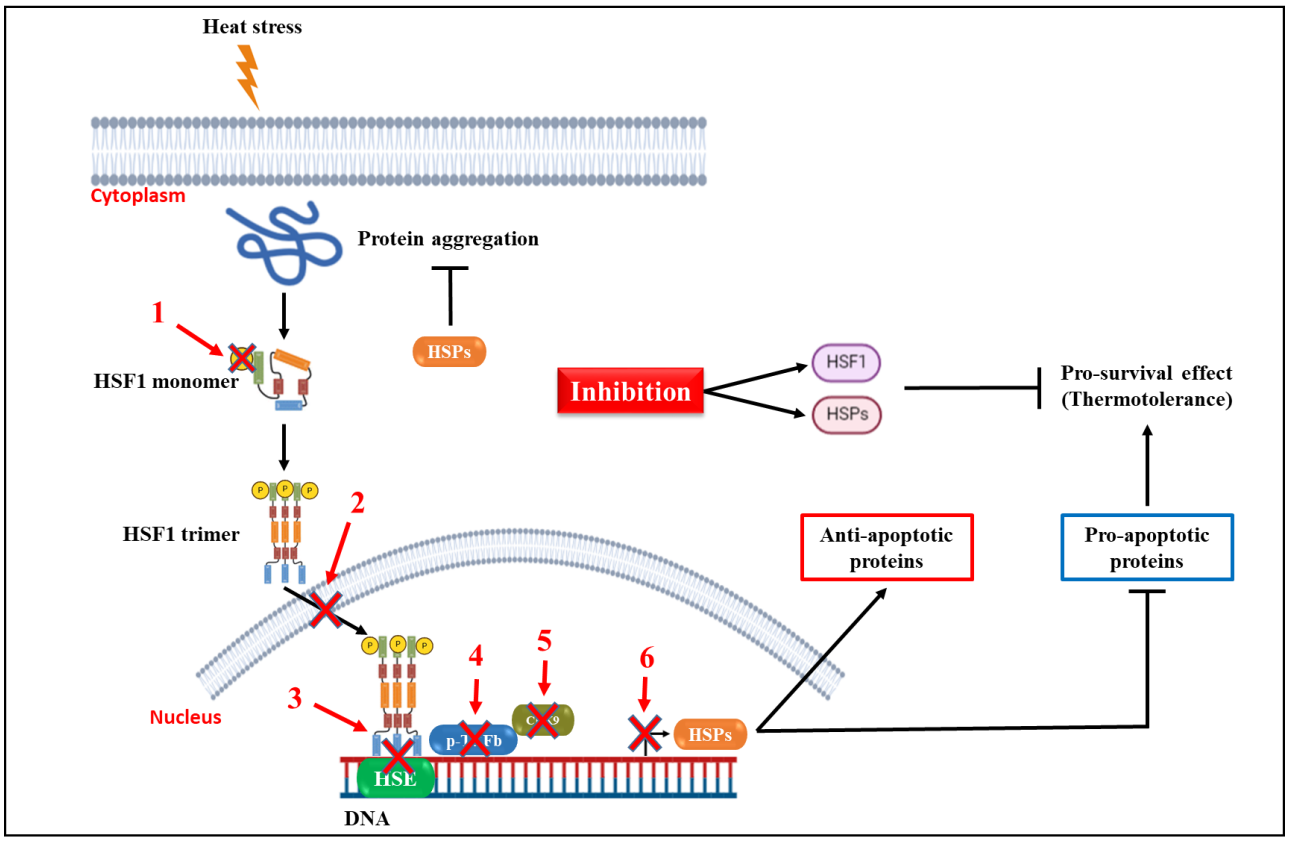

Figure 4. Mechanism of action of HSF1 inhibitors. Various HSF1 inhibitors target distinct steps in the HSF1 pathway: 1) Emunin and PW3405 inhibit HSF1 phosphorylation, reducing its activation. 2) Dorsomorphin and Resveratrol prevent HSF1 from translocating into the nucleus. 3) Quercetin, fisetin and curcumin, suppress HSF1's ability to bind the HSE. 4) KRIBB11 and cantharidin block HSF1-dependent recruitment of the positive transcription elongation factor (p-TEFb), which impede downstream effects. 5) CDK9 inhibitors, such as 4,6-disubstituted pyrimidines, indirectly hinder HSF1 function. 6) CCT251236 and BEZ235 directly inhibit HSF1-mediated transcriptional activity. The HSF1 inhibition mechanism is still not clear for two compounds: CL-43 and SNS-032. Graphical design based on Ahmed *et al.* (18). Published by Viana *et al.* (25). Created with biorender.com.

1.4.2. mEHT and the HSF1 inhibitors

As HSF1 plays a remarkable role in tumorigenesis, its knockdown may reduce the proliferation, migration and invasion of cancer cells (43, 144), hence the development of HSF1 and HSP inhibitors became a target of cancer research (145). While mEHT activates protective mechanisms, particularly through inducing heat shock proteins like HSP70, its anti-cancer efficacy may be improved by inhibiting the HSP-mediated defense mechanisms of cancer

cells (90). Therefore, targeting HSF1 domains with small molecules may have favorable outcomes profile.

Several potential inhibitors of HSF1 have been formulated, commonly derived from either natural products or synthetic chemical structures. Recent reviews provide detailed overview of the currently available compounds, their structure and mode of action (35, 43, 143, 146, 147) (**Figure 4**). Some of these compounds were used in combination with mEHT. Kuo *et al.* verified that combining curcumin and resveratrol with mEHT increased immune cell infiltration into malignant tumors (140). In turn, HSP70 overexpression was also reported in cancers treated with this combined therapy. However, the authors proposed a mechanism by which HSP70 mediates antigen-presenting cells recruitment, leading to enhanced anti-cancer efficacy in CT26 malignant tumors (140).

1.4.3. KRIBB11

KRIBB11 (N^2-(1*H*-indazole-5-yl)-N^6-methyl-3-nitropyridine-2,6-diamine) is a small molecule inhibitor that has gained significant attention in cancer research due to its ability to target the HSR pathway. Unlike other HSR inhibitors, KRIBB11 specifically targets HSF1, the master regulator of the HSR. It exerts its inhibitory effects by disrupting the binding of the Positive Transcription Elongation Factor b (p-TEFb) to the promoter region of the HSP gene (148). KRIBB11 has been reported to inhibit HSF1 expression in pancreatic cancer (69), breast cancer (149-151), and also triple-negative breast cancer (152), bladder cancer (153), lung cancer (154), hepatocellular carcinoma (155), myeloma cells (156), glioblastoma cells (157), and leukemia model (158). These *in vivo* experiments have demonstrated that KRIBB11 can reduce cancer growth without significant body weight loss or toxicity (148, 150, 153, 155, 156, 158). Additionally, KRIBB11 has been shown to disrupt the HSF1-HSP interaction, preventing the transcriptional activation of HSP genes (153, 154, 156-158). Notably, KRIBB11 was reported to inhibit the expression of HSP70 under heat shock (148). Contrarily, Yoo *et al.* results were inconsistent with those previous studies that demonstrated KRIBB11 anticancer effect

through HSF1 depletion. In fact, this group failed to prove the downregulation of HSF1 and HSPs by KRIBB11, indicating that the activation of different molecular pathways by KRIBB11 depends on the application of the compound whether in a steady state or under stress conditions, such as heat shock, which could potentially result in the HSF1 activation (159). The inhibition of the HSR, however, is of particular interest in cancer therapy, as the HSR plays a crucial role in promoting cancer cell survival and resistance to various stressors, including hyperthermia (27). All together, these results suggest that KRIBB11 might have high translational potential.

In vitro experiments demonstrated that KRIBB11 when applied in combination with mEHT treatments not only reduced breast cancer cell viability but also inhibited HSP70 mRNA upregulation normally seen in mEHT monotherapy (90). Moreover, the mEHT + KRIBB11 synergism was also proposed to decrease the heat shock-related complement production through C4b, an acute phase protein (89).

1.5. Progesterone Receptor

Progesterone receptors (PGR) are members of the nuclear/steroid receptor family, functioning as ligand-dependent transcription factors, that are expressed primarily in female reproductive tissues and in the central nervous system (160, 161). When bound to the ovarian steroid ligand progesterone, PGR becomes activated and translocates to the nucleus. There, it binds to specific sites in the DNA known as Progesterone Response Elements (PREs), thereby regulating the expression of target genes (162).

In normal human tissues where the receptor is normally expressed, including the breast, PGR behaves as a key regulator of epithelial cell proliferation, differentiation, and tissue homeostasis, contributing to the cyclical changes observed during the menstrual cycle and supporting overall breast health (163).

1.5.1. Progesterone Receptor and Breast Cancer

Progesterone, a vital female hormone, is increasingly recognized for its role in cancer development and progression (164). Consequently, the scientific community is placing significant attention on understanding the involvement of progesterone in breast and gynecological cancers (165). Indeed, elevated levels of PGR have been associated with increased transcription of specific genes involved in cell proliferation and metastasis (166), leading to a poorer prognosis and resistance to chemotherapy (161). Consequently, PGR is routinely utilized as a biomarker for characterizing breast cancer at diagnosis (163). On the other hand, malignant tumors expressing PGR respond more effectively to antiprogestins, which are drugs that counteract the effects of progesterone (160). Mifepristone (MIF), for instance, is known to inhibit cell proliferation in cancers that overexpress progesterone receptor isoform A (PRA), a PGR isoform observed in breast cancer that promotes tumor growth and progression (167). MIF, together with Ulipristal Acetate (UPA), is included in a new class of synthetic steroid ligands known as Selective Progesterone Receptor Modulators (SPRMs) that have been used to compete at the PGR-target site in a tissue-specific manner, thereby inhibiting the proliferation of breast cancer cells (161, 168, 169).

While the presence of PGR in primary breast carcinomas is typically regarded as a marker of a favorable prognosis, correlating with better overall survival rates, PGR-negative cancers tend to exhibit lower differentiation and are associated with more aggressive cancer types (170). This association is supported by numerous clinical studies and meta-analyses, which consistently demonstrate that patients with PGR-positive breast cancers have superior clinical outcomes compared to those with PGR-negative cancers (171-174). The positive prognostic impact of PGR expression lies in its role in regulating essential biological processes linked to cancer development and progression, and responding to endocrine therapy.

2. Objectives

The studies summarized in this thesis investigated molecular mechanisms of modulated electro-hyperthermia (mEHT) and their anti-cancer potential in Triple-Negative Breast Cancer (TNBC) *in vitro* and *in vivo* mouse model, including:

- To establish a 4T1 cell model *in vitro* using a CRISPR/Cas9 lentiviral construct to knockdown Heat Shock Factor 1 (HSF1) gene;
- To investigate the impact of HSF1 downregulation on the Heat Shock Response (HSR) subsequent to mEHT treatments *in vivo*;
- To evaluate the combined therapeutic impact of mEHT and HSF1 inhibition with KRIBB11 inhibitor *in vivo*;
- To explore the modulation of HSP70 in response to mEHT in combination with either HSF1 knockdown or KRIBB11 treatment;
- To elucidate the alterations in Progesterone Receptor (PGR) expression in response to *in vivo* mEHT treatments using a comprehensive multiplex analysis at the mRNA level;
- To verify the changes in PGR expression at the protein level;
- To evaluate the potential synergistic effect of combining mEHT treatments with antiprogestins, Mifepristone (MIF) or Ulipristal Acetate (UPA), on the viability of 4T1 TNBC cells;
- To evaluate how effective is to combine MIF or UPA with mEHT treatments, as opposed to combining these antiprogestins with conventional hyperthermia *in vitro*.

3. Materials and Methods

3.1. Cell Culture and Reagents

For both *in vitro* and *in vivo* studies, the 4T1 murine mammary carcinoma cell line was used. The 4T1 cell line is a widely used murine breast cancer cell line known for its aggressive metastatic behavior in immunocompetent syngeneic mouse models. It is isogenic, meaning it shares identical genetic background with the host, facilitating the study of immune-cancer interactions without rejection. The 4T1 cells were grown as adherent culture in Dulbecco's Modified Eagle Medium (DMEM high glucose, 4.5 g/L without L-glutamine and Phenol Red, Capricorn Scientific, Ebsdorfergrund, Germany, Cat-No. DMEM-HXRXA) supplemented with 10% Fetal Bovine Serum (FBS – South America Origen, EU approved, EuroClone S.p.A., Pero, Italy, Cat-No. ECS0180L), L-glutamine 200 mM (Capricorn Scientific, Ebsdorfergrund, Germany, Cat-No. GLN-B), and penicillin/streptomycin 100x (Capricorn Scientific, Ebsdorfergrund, Germany, Cat-No. PS-B). Cells were submitted to passages every 2 or 3 days. Trypsin 10x (Lonza A. G., Basel, Switzerland, Cat-No. 17-160E) was used to release cells from sub-confluent monolayers. The detached cells were seeded back into cell culture flasks or prepared for experiments. KRIBB11 was purchased from MedChemExpress (MCE®, Monmouth Junction, NJ, USA, Cat-No. HY-100872). Mifepristone (Cat-No. HY-13683) and Ulipristal Acetate (Cat-No. HY-16508) were purchased from MedChem Express (MCE®, Monmouth Junction, NJ, USA).

3.2. Cell Viability Assay

The viable yield was determined by resazurin assay method, as described (175). Resazurin is a cell permeable redox indicator used to monitor cytotoxic effects that eventually lead to cell death. In this way, viable cells with active metabolism can reduce resazurin into the resofurin product, giving a pink fluorescent color (175). High purity resazurin sodium salt (Sigma-Aldrich Co., St. Louis, MO, USA, Cat-No. R7017) was dissolved in PBS (without Ca & Mg, without Phenol Red, Capricorn Scientific, Ebsdorfergrund, Germany, Cat-No.

PBS-1A) to 0.3 mg/ml concentration and filtered through a 0.2 μm filter. After aspirating the residual media, working solutions containing 10% (v/v) resazurin stock solutions diluted in culture media were added to each well and incubated for 2 hours in humidity chamber (5% CO_2 at 37°C). Fluorescence was recorded at 560 nm excitation / 590 nm emission filter set using a microplate reader (BioTek PowerWave HT 340 Microplate Reader, Bad Friedrichshall, Germany).

3.3. Cell Proliferation

Cell growth was evaluated in the 4T1 TNBC cell line that was subjected to dose-response treatments with mifepristone (MIF) or ulipristal acetate (UPA). To measure proliferation in the presence of MIF or UPA, cells were seeded into 96-well plate at a density of 5 x 10^3 cells/well which ensured exponential growth while preventing the cells from reaching 100% confluence over the course of the experiment. Following a period of 24 hours allotted for adherence, the cells were cultured in the continuous presence of MIF or UPA for 72 hours at doses of 0, 5, 10, 15, 20, 25, 30, 35, and 40 μM. Control groups of cells were treated with vehicle DMSO (Sigma-Aldrich Co., St. Louis, MO, USA, Cat-No. D2438) at a final concentration of 0.01%. Culture media containing resazurin as described above was added to triplicate cultures. When indicated, the concentration of MIF or UPA required to inhibit cell proliferation by 50% or IC_{50} were determined using GraphPad Prism software (v.6.01; GraphPad Software, Inc., La Jolla, CA, USA).

3.4. Construction and verification of stable HSF1-knockdown by flow cytometry

CRISPR Guide RNA (gRNA) Lentiviral Transduction particles from Sigma-Aldrich® (St. Louis, MO, USA) was used for knockdown of HSF1. The plasmid sequences for HSF1 gene are listed in **Figure 5**. The lentiviral structure consisted of 1) the target region to knockdown HSF1-gene; 2) a puromycin resistance gene; and 3) Green Fluorescent Protein (GFP) gene. Murine 4T1 cells were seeded at 1.4 x 10^4 cells/well in triplicate into a 96-well plate and

incubated for 24 hours at 37 °C. After the cells were adherent to the bottom, 8 µg/mL of hexadimethrine bromide (Sigma-Aldrich/Merck, St. Louis, MO, USA, Cat-No. H9268-5G) were added to each well to enhance transduction. The lentiviral particles or the negative particles were added to appropriate wells. Cells were further cultured for 24 hours, and then the medium containing the lentiviral particles were replaced. Next, transfected cells were selected by culturing in a medium containing 6 µg/ml puromycin (Sigma-Aldrich/Merck, St. Louis, MO, USA, Cat-No. 540411-25MG) to kill non-transfected cells as established earlier (90). Surviving cells were considered successfully transfected cells. Forty-eight hours after transduction, fluorescence of successful transduced cells was assessed by fluorescent microscope. Puromycin-resistant colonies were selected and expanded to assay for expression of the construct. Cells were sorted by Fluorescence-activated single cell sorting (FACS) (Sony Corp. San Jose, CA, USA, Sony SH800) in three cell types: 4T1 wild type, 4T1 empty vector, and 4T1 HSF1-KO. Flow cytometry was used to check for GFP-positiveness in transduced cells after expansion. For that, cells were harvested at 1 x 10^6 cells/mL, washed with cold PBS, and centrifuged for 5 minutes at 300 g. The supernatant was removed, and fresh, cold PBS was added. The suspended cells were transferred to FACS tubes and were kept on ice. Cells were analyzed based on GFP-expression by using a CytoFLEX Flow Cytometer (Beckman Coulter, Inc. Brea, CA, USA).

A

Vector	Clone ID	Digest	Pasmid sequence verified	P24 antigen ELISA titer ≥ 10^6 VP/ml
LV01	NEGATIVECONTROL1	PASS	CGCGATAGCGCGAATATATT	3.7x10^7 VP/mL
LV01	MMPD0000018544	PASS	GCTCGCCTCCAGTACCCGA	1.6x10^7 VP/mL

B

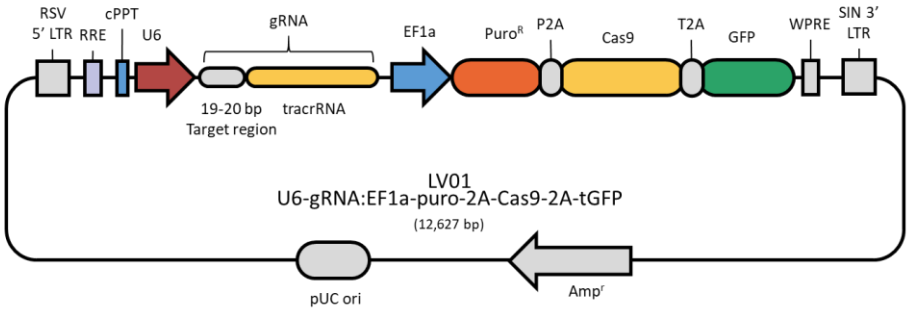

Figure 5. CRISPR/Cas 9 lentiviral constructs. A) Plasmid sequence of the negative control (empty vector) and the HSF1 knockdown, which contains the target gene. **B)** Scheme showing the structure of HSF1-KO lentiviral particles. Modified from Sigma-Aldrich® (St. Louis, MO, USA). Published by Viana *et al.* (176).

3.5. *In vitro* HSF1-KO model

Knockdown-, empty vector-, and wild type 4T1 cells were counted and seeded onto 60 mm petri dishes at a density of 1 x 10^6 cells per petri dish in DMEM medium with 10% FBS. After 24 hours, cells were treated with water bath hyperthermia, 42°C for 30 minutes. Two hours after hyperthermia treatment, the medium was discarded and 500 µL TRI Reagent® RT (Molecular Research Center, Inc. Cincinnati, OH, USA, Cat-No. RT 111) was added for RNA collection. The cells were homogenized and transferred to pre-labeled Eppendorf tubes. The Eppendorf tubes were immediately frozen in liquid nitrogen. The protocol was continued as described in 3.8. section.

3.6. *In vivo* HSF1-KO model

Six-to-eight-weeks old female BALB/c mice were kept under 12 hours' dark/light cycles with *ad libitum* access to food and water in the Animal Facility Department of Basic Medical Center (Semmelweis University, Budapest, Hungary). The mice were anesthetized with isoflurane (Baxter International Inc., Deerfield, IL, USA). Anesthesia was induced with 5% concentration and

maintained with 2-2.5% concentration in 0.6–0.8 l/min compressed airflow. 4T1 cells were kept in cell culture flasks, trypsinized, counted, suspended in Dulbecco's PBS. 1×10^6 4T1 cells suspended in 50 µL PBS were subcutaneously inoculated into the 4th mammary gland's fat pad of each mouse as described by Zhang *et al.* (177) using a 50 µL Hamilton syringe (Hamilton Company, Reno, NV, USA). Eight days after inoculation, tumor size was measured with digital caliper (Fine Science Tools lnc., Foster City, CA, USA) and ultrasound (Phillips Sonos 5500, Philips, Amsterdam, Netherlands) as described earlier (90). Mice were randomized into treatment groups according to their tumor volume and body weight, to achieve similar average for all groups. Animals exhibiting disproportionate tumor measures, such as irregular shapes, twin tumors, or those where the size significantly deviated from the average, were excluded from the experiment. In total, four mEHT treatments were performed every two days. In the days between treatments, tumor size was measured by both digital caliper and ultrasound. **Figure 6** shows a schematic overview of HSF1-KO and mEHT treatments schedule. Mice were kept under isoflurane anesthesia for all procedures described above. For tumor sample collection 24 hours after the last treatment, heparin 10x (Teva, Debrecen, Hungary, Cat-No. OGYI-T-2216/01) was injected intraperitoneally. Mice physical body condition was checked, and mice were terminated by cervical dislocation. The abdominal cavity was opened, blood was taken, and tumors were harvested, cleaned (from adjacent connective tissues), weighed, and halved in two similar halves: one half was placed in 4% formaldehyde solution (Semmelweis Pharmacy, Budapest, Hungary) and sent to histological processing; the other half was frozen in liquid nitrogen for molecular analysis. Interventions and housing of the animals conformed to the Hungarian Laws No. XXVIII/1998 and LXVII/2002 about the protection and welfare of animals, and the directives of the European Union. All animal procedures were approved by the National Scientific Ethical Committee on Animal Experimentation under the No. PE/EA/50-2/2019.

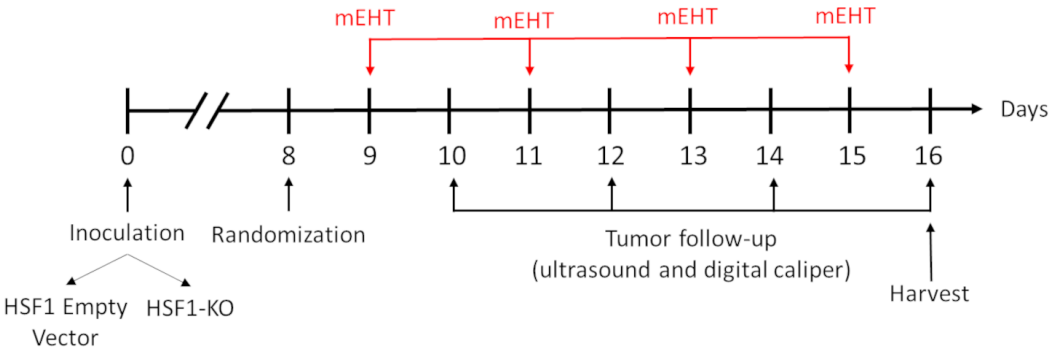

Figure 6. Experimental scheme of the 4T1 HSF1 knockdown model. 4T1 TNBC cells, containing either the HSF1 empty vector (EV) lentiviral construct or the HSF1 knockdown (HSF1-KO) lentiviral construct, were inoculated at day zero. Mice were randomized into groups (Sham EV or mEHT EV, and Sham HSF1-KO or mEHT HSF1-KO) at day 8. mEHT treatments were performed every two days. Tumor volume was monitored by ultrasound and digital caliper between mEHT treatments. The study was terminated on day 16 with the harvest of tumors. Published by Viana *et al.* (176).

3.7. *In vivo* KRIBB11 model

KRIBB11 (MedChemExpress, Monmouth Junction, NJ, USA, Cat-No. HY-100872) was dissolved in 10% dimethylacetamide (MedChemExpress, New Jersey, USA, Cat-No. HY-W042416), 50% PEG300 (MedChemExpress, Monmouth Junction, NJ, USA, Cat.No.: HY-Y0873), and 40% nuclease-free water (Invitrogen, Carlsbad, CA, USA, Cat-No. 10977-035), as described previously (148). Following randomization as described above, KRIBB11 was administrated intraperitoneally at a dose of 50 mg/kg/day for 8 days. **Figure 7** depicts a schematic overview of mEHT + KRIBB11 experiment. Tumor volume was followed as described above. In total, four mEHT treatments were performed every two days. On day 16, the mice were sacrificed, and the tumors were removed, halved, and analyzed by immunohistochemistry (IHC) and qRT-PCR.

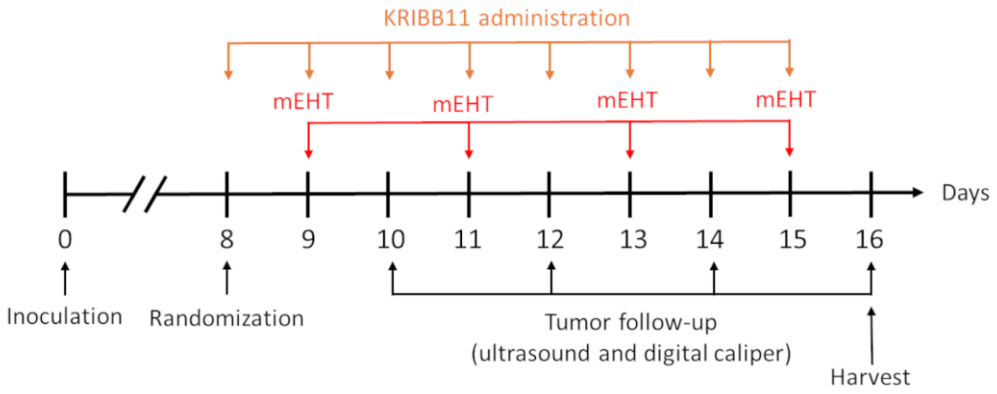

Figure 7. Experimental scheme of the mEHT + KRIBB11 experiment. 4T1 Wild Type (WT) cells were inoculated at day zero. Mice were randomized into groups at day 8 together with the first KRIBB11 injection. KRIBB11 was administered every day for 8 days. mEHT treatments were performed every two days. Tumor volume was monitored by ultrasound and digital caliper between mEHT treatments. The study was terminated on day 16 with the harvest of tumors. Published by Viana *et al.* (176).

3.8. *In vitro* mEHT Treatments

An *in vitro* heating model was established using the LabEHY *in vitro* applicator (Oncotherm Ltd., Budaörs, Hungary) within an electrode chamber (**Figure 8**). This *in vitro* setup was introduced previously by our group (90). Wild Type 4T1 cells were counted and seeded onto 35 mm petri dishes at a density of 2 x 10^5 cells per petri dish in DMEM with 10% FBS. The cells were allowed to grow overnight in a humidity chamber (5% CO_2 at 37°C). After 24 hours, the cells were placed in a plastic bag immersed in distilled water in the mEHT chamber, maintaining a temperature of 42°C for 30 minutes. Temperature monitoring utilized the TM-200 thermometer (Oncotherm Ltd., Budaörs, Hungary), with an average power of 4 ± 1 watts applied. For the conventional hyperthermia control, the cell suspension was placed in a microtube with culture medium and incubated at 42°C for 30 minutes in a water bath (ThermoFisher Scientific, Waltham, MA, USA, Cat-No. TSGP02). Treated cells at a density of 5 x 10^3 cells/well were transferred to 96-well plates and allowed to adhere to the bottom for 6 hours. Subsequently, the cells were incubated with either mifepristone or ulipristal acetate at 30 or 35 µM, respectively, or 0.01% DMSO. After twenty-four hours, cell viability was assessed using the resazurin assay, as described in section 3.2.

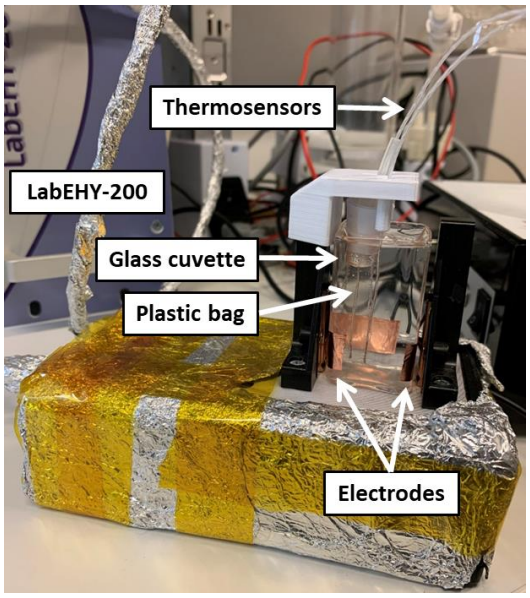

Figure 8. Modulated electro-hyperthermia (mEHT) treatment setup with LabEHY-200 applicator designed for *in vitro* experiments. Cancer cells enclosed in a plastic bag are positioned within a cuvette, filled with distilled water. Copper electrodes induce the electromagnetic field and heat generation. Temperature sensors inside the bag and cuvette enable temperature monitoring throughout the treatment process. Published by Viana *et al.* (176).

3.9. *In vivo* mEHT Treatments

Tumor-bearing mice were treated with modulated electro-hyperthermia (mEHT) device as described in detail earlier (89). Briefly, electromagnetic heating was generated by capacitive coupled, amplitude modulated 13.56 MHz radiofrequency electromagnetic field (LabEHY 200, Oncotherm kft., Budaors, Hungary). The mice were mEHT-treated four times every two days for 30 minutes plus maximum 5 minutes for device stabilization with applied energy that varied between 0.2 and 1.0 watts. Temperature monitoring was performed with optical sensors (Luxtron FOT Lab Kit, LumaSense Technologies, Inc., CA, USA). The optical sensors were calibrated before each treatment and were placed: on the skin right above the tumor, into the rectum for body temperature monitoring, on the heating pad, and near the treatment setup for room temperature monitoring. The skin temperature was kept at 40 ± 0.5 °C during the treatments, as it assured the required 42°C inside the tumor. Rectal temperature was kept in the physiologic range (37.0 ± 0.5 °C), and the heating

pad was set at the same temperature. Room temperature was 25 ± 1 °C. For sham treatments, cables were disconnected, therefore, no electromagnetic field was generated, and no energy was transferred (no heating).

3.10. Histopathology and Immunohistochemistry

Formalin-fixed cancer samples were dehydrated and embedded in paraffin. Serial sections (2.5 μm) were cut for hematoxylin-eosin (H&E) staining or dewaxed and rehydrated for immunohistochemistry (IHC) using a polymer-peroxidase system (Histols, Histopathology Ltd., Pécs, Hungary). H&E and stained slides were digitalized using Pannoramic Scan and analyzed with the HistoQuant module of CaseViewer image-analysis software (all from 3DHISTECH, Budapest, Hungary) based on image color and intensity segmentation. The tumor area was digitally annotated and the damaged and living areas were delimited. The ratio between the damaged area per the whole tumor area was used for calculating the tumor destruction ratio (TDR%) on H&E slides.

$$\textbf{TDR (\%)} = \frac{\textbf{Damaged area}}{\textbf{Whole tumor area}}$$

Slide samples used in IHC were deparaffinized and incubated for 20 minutes with 3% H_2O_2 in methanol to block endogenous peroxidase activity. For antigen retrieval, slide samples were soaked in citrate buffer and heated for 20 minutes using an Avair electric pressure cooker (ELLA 6 LUX (D6K2A), Bitalon Kft, Pécs, Hungary), followed by 30 minutes cooling step in 3% bovine serum albumin (BSA, Millipore Corp., Kankakee, IL, USA, Cat-No. 82-100-6) solution was used to block non-specific proteins for 20 minutes. The sections were incubated with the primary antibodies diluted in 1% BSA/TBS + TWEEN (TBST, pH 7.4) (**Table 1**) overnight in humidity chamber. Peroxidase-conjugated anti-rabbit & anti-mouse IgGs (HISTOLS-MR-T, micropolymer - 30011.500T, Histopathology Ltd., Pécs, Hungary) were used for 40 min incubation and the enzyme activity was revealed in 3, 3'-diaminobenzidine (DAB) chromogen/hydrogen peroxide kit (DAB Quanto-TA-060-QHDX-

Thermo Fischer Scientific, Waltham, MA, USA, Cat-No. 12623957) under optical microscope. All incubations were at room temperature with sample washings between incubations in TBST buffer for 3 × 5 min. Slides were digitalized and the reactions were evaluated. The tumor area was digitally annotated and the area containing positive immune reaction was masked by setting the intensity, color, and saturation in the annotated area on each staining using the QuantCenter module of CaseViewer. The ratio of the masked area to the annotated area (relative mask area = rMA) was used to estimate the expression of the target molecule. rMA of HSF1, HSP70, and PGR were measured in the intact tumor area. Important to mention, due to technical problems there is no data about HSP70 staining of three samples from KRIBB11 experiment: one in Sham vehicle, one in Sham KRIBB11, and one in mEHT KRIBB11.

Table 1. Antibodies and conditions used for immunohistochemistry

Antigen	Type	Reference no.	Dilution	Vendor[1]
HSF1	Rabbit, pAb	#4356	1:100	Cell Signaling
HSP70	Rabbit, pAb	#4872	1:100	Cell Signaling
PGR	Mouse, pAb	# MA1-410	1:100	Thermo

[1]Vendor specifications: Cell Signaling (Danvers, MA, USA)

3.11. RNA Isolation and mRNA RT-PCR

RNA was isolated with the TRI reagent® RT (Molecular Research Center lnc., Cincinnati, OH, USA, Cat-No. RT111) according to the manufacturer's instructions. RNA integrity was analyzed by agarose gel electrophoresis, sample purity and concentration were measured by a Nanodrop spectrophotometer (Thermo Fisher Scientific Inc., Waltham, MA, USA). Reverse transcription of isolated RNA was performed by High-Capacity cDNA Reverse Transcription Kit (Applied Biosystems Inc., Foster City, CA, USA, Cat-No. 4368814). The amplified cDNA was used as a template for RT-PCR. Gene expression was measured according to standard qPCR procedures with SYBER Green based RT-PCR with SsoAdvanced™ Universal SYBER® Green Supermix (Bio Rad Laboratories, Inc., Hercules, CA, USA, Cat-No.

1725271) on CFX Connect Real-Time PCR Detection System (Bio Rad Laboratories, Inc., Hercules, CA, USA). The relative expression values for the target mRNAs were calculated after normalization using GAPDH. The primers used are listed in **Table 2**.

Table 2. Primers used for RT-PCR

Gene Symbol	Gene Name	Primer Pairs
GAPDH	Glyceraldehyde-3-phosphate-dehydrogenase [*Mus musculus*]	Fwd: CTCCCACTCTTCCACCTTCG Rev: GCCTCTCTTGCTCAGTGTCC
HSP70	Heat shock protein 70 [*Mus musculus*]	Fwd: CTTCACCTCCAAGTTCACCAA Rev: GACTCTGCTGCTTCTCCTTG
HSF1	Heat shock factor 1 [*Mus musculus*]	Fwd: CTGAGAAGTGCCTCAGCGTA Rev: CTCCTGAATGTCCAGCAGGG
PGR	Progesterone receptor [*Mus musculus*]	Fwd: GTGCTTACCTGTGGGAGCTG Rev: ACGACATGCTGGGCAGTTTT
RPLP0	Ribosomal protein lateral stalk subunit P0 [*Mus musculus*]	Fwd: GATTCGGGATATGCTGTTGG Rev: GTTCTGAGCTGGCACAGTGA

3.12. Next-Generation Sequencing and Bioinformatic Analysis

NGS technique was described by our group (89). Shortly, eight tumor samples, four sham and four mEHT-treated, were selected based on the quality and quantity of isolated RNA. RNA integrity and RNA concentration were assessed by the RNA ScreenTape system with the 2200 Tapestation (Agilent Technologies, Santa Clara, CA, USA) and the RNA HS Assay Kit with the Qubit 3.0 Fluorometer (ThermoFisher Scientific, Waltham, MA, USA, Cat-No. Q32852). Library preparation and sequencing followed standard protocols. Reads were aligned to the *Mus musculus* reference genome (GRCm38, STAR v2.6.1c). Differential expression (DE) analysis used FC > 2.0 and *p*-value < 0.05 thresholds.

3.13. NanoString Analysis

NanoString technology application in 4T1 mouse model was used by our group (89). The same samples used for NGS were also used for NanoString. Qubit 4 Fluorometer (Thermo Fisher Scientific, Waltham, MA, USA, Cat-No. Q33238) was used to measure RNA concentrations. Total RNA was hybridized

to the customized nCounter® gene panel (NanoString, Redwood, CA, USA). The applied custom gene panel was composed by 134 genes, including PGR, identified as differentially expressed (highest FC and lowest *p* values) by NGS. Samples were transferred to the nCounter Prep Station for further processing. The gene expression profiles of the samples were digitalized with the nCounter Digital Analyzer. Quality assessment and normalization were performed in nSolver 4.0 Analysis Software (NanoString, Redwood, CA, USA). Background was determined with synthetic negative probes provided by the NanoString company.

3.14. Statistical Analysis

All statistical analyses were performed using the statistical software program GraphPad Prism software (v.6.01; GraphPad Software, Inc., La Jolla, CA, USA). Differences between groups were assessed using the following methods: One-way ANOVA for comparisons involving more than two groups, Two-way ANOVA for longitudinal measurements (such as tumor volume), and t-tests for comparing sham-treated and mEHT-treated groups. Differences were considered statistically significant at * $p < 0.05$, ** $p < 0.01$, *** $p < 0.001$, **** $p < 0.0001$, ns = not significant. Data are given as mean ± Standard Deviation (SD).

4. Results

4.1. Successful transduction of 4T1 cell line with the HSF1-gene editing lentiviral construct

The HSF1-knockdown (HSF1-KO) CRISPR/Cas9 construct included a GFP encoding sequence for the selection of transfected cells. As expected, non-transduced wild type (WT) 4T1 cells did not express GFP (**Figure 9A**). In contrast, more than 95% of 4T1 cells transduced with the active HSF1-KO CRISPR/Cas9 construct successfully expressed GFP, confirming successful transduction (**Figure 9C**). Transduction with the empty vector (EV) was less effective, resulting in 62.8% of cells being GFP-positive, while 37.2% remained non-transduced (**Figure 9B**).

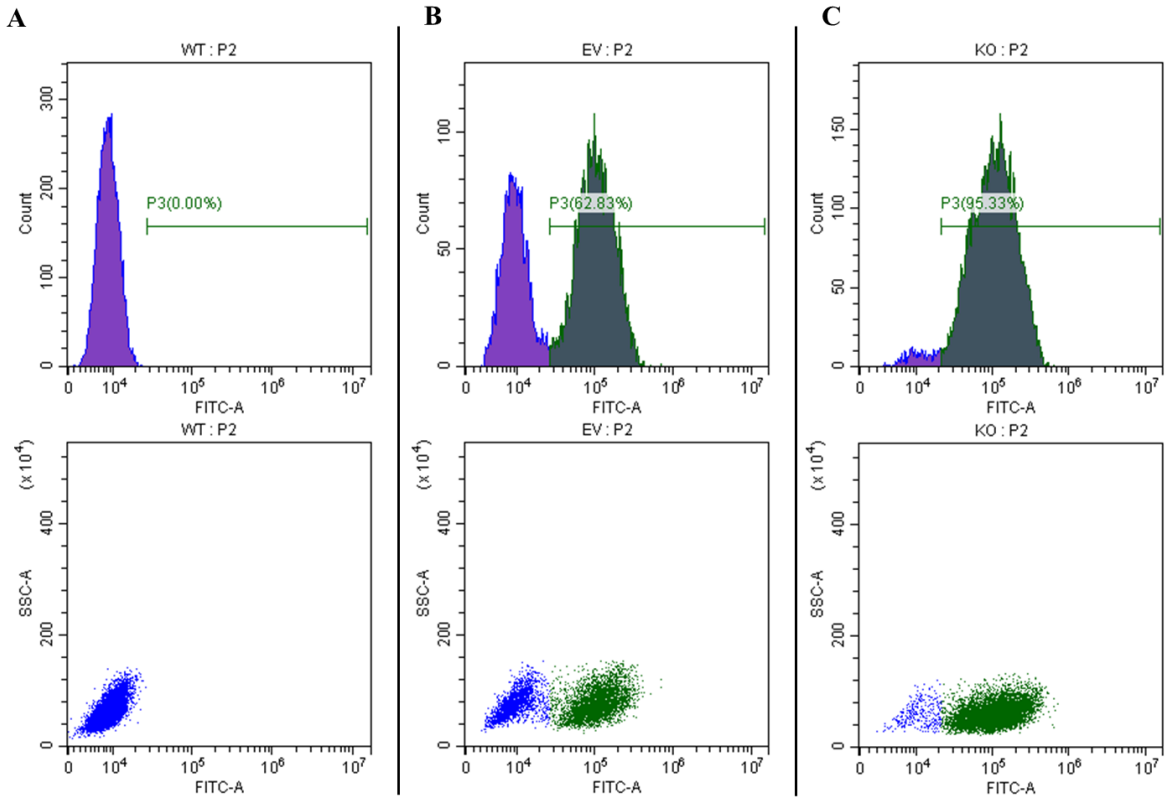

Figure 9. Flow cytometric analysis of transfected 4T1 cells. Flow cytometry histograms (upper row) and dot plots (lower row). **A)** Wild Type (WT); **B)** Empty Vector (EV); and **C)** HSF1-KO (KO). The GFP positive cells are indicated with green, and the GFP-negative population with blue. SSC: Side Scatter; P2: second gate; FITC: Fluorescein Isothiocyanate. Published by Viana *et al.* (176).

4.2. Successful reduction of HSF1 and HSP70 expression in transduced TNBC cell line

HSF1 mRNA levels were comparable in both WT and EV cells, whether maintained at 37°C or exposed to 42°C in cell culture (**Figure 10A**). Notably, the lentiviral construct led to a substantial downregulation of HSF1 mRNA in the knockdown group (HSF1-KO), as compared to both the wild type and empty vector groups (**Figure 10A**). Baseline expression of HSP70 at 37°C remained low across all groups (**Figure 10B**). Elevating the culture temperature to 42°C significantly induced HSP70 upregulation in WT and EV cells. However, this heat-induced response was significantly diminished in the HSF1-KO group (**Figure 10B**).

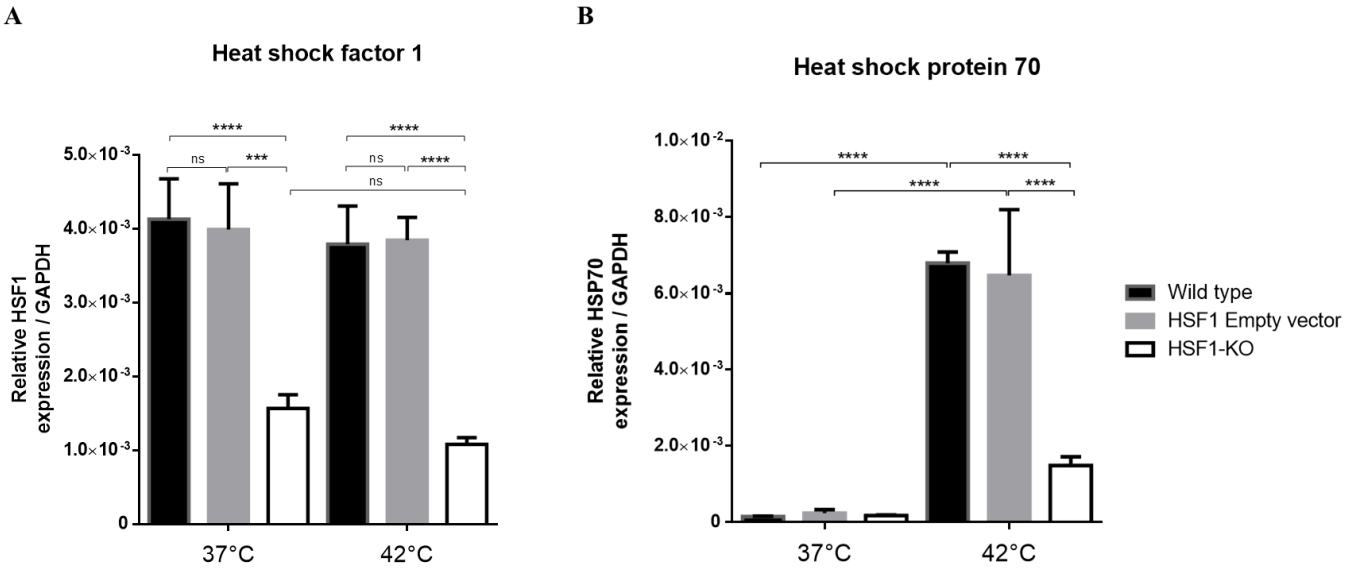

Figure 10. HSF1 and HSP70 mRNA relative expression at 37°C and 42°C in the 4T1 cell line. **A)** HSF1; **B)** HSP70. GAPDH: Glyceraldehyde 3-phosphate dehydrogenase: housekeeping gene. One-way ANOVA, Mean ± SD, n = 3/group, ns = not significant, *** $p < 0.001$, **** $p < 0.0001$. Published by Viana *et al.* (176).

4.3. mEHT-induced tumor growth reduction was enhanced in HSF1-KO tumors

The Sham EV tumors nearly doubled in volume over the course of the experiment (**Figure 11A, B** - red). In contrast, Sham HSF1-KO were smaller and their growth rate was slower than EV tumors (rose). Remarkably, mEHT

treated tumors did not grow and their size was reduced after the 4th treatment. The tumor growth rate measured by caliper was significantly slower in the HSF1-KO mEHT-treated group (light blue) compared to mEHT treated EV group (dark blue). Despite having similar initial tumor volumes, mEHT KO tumors were notably smaller than mEHT EV tumors by the end of the study. Furthermore, supporting the tumor volume data, tumor mass was reduced by both mEHT and HSF1-KO; yet, the smallest tumors were observed in the mEHT KO group (**Figure 11C, D**) by the study termination. This reinforces the reliability of the tumor size measurements, as tumor volume strongly correlated with tumor mass during follow-up (**Figure 11E, F**).

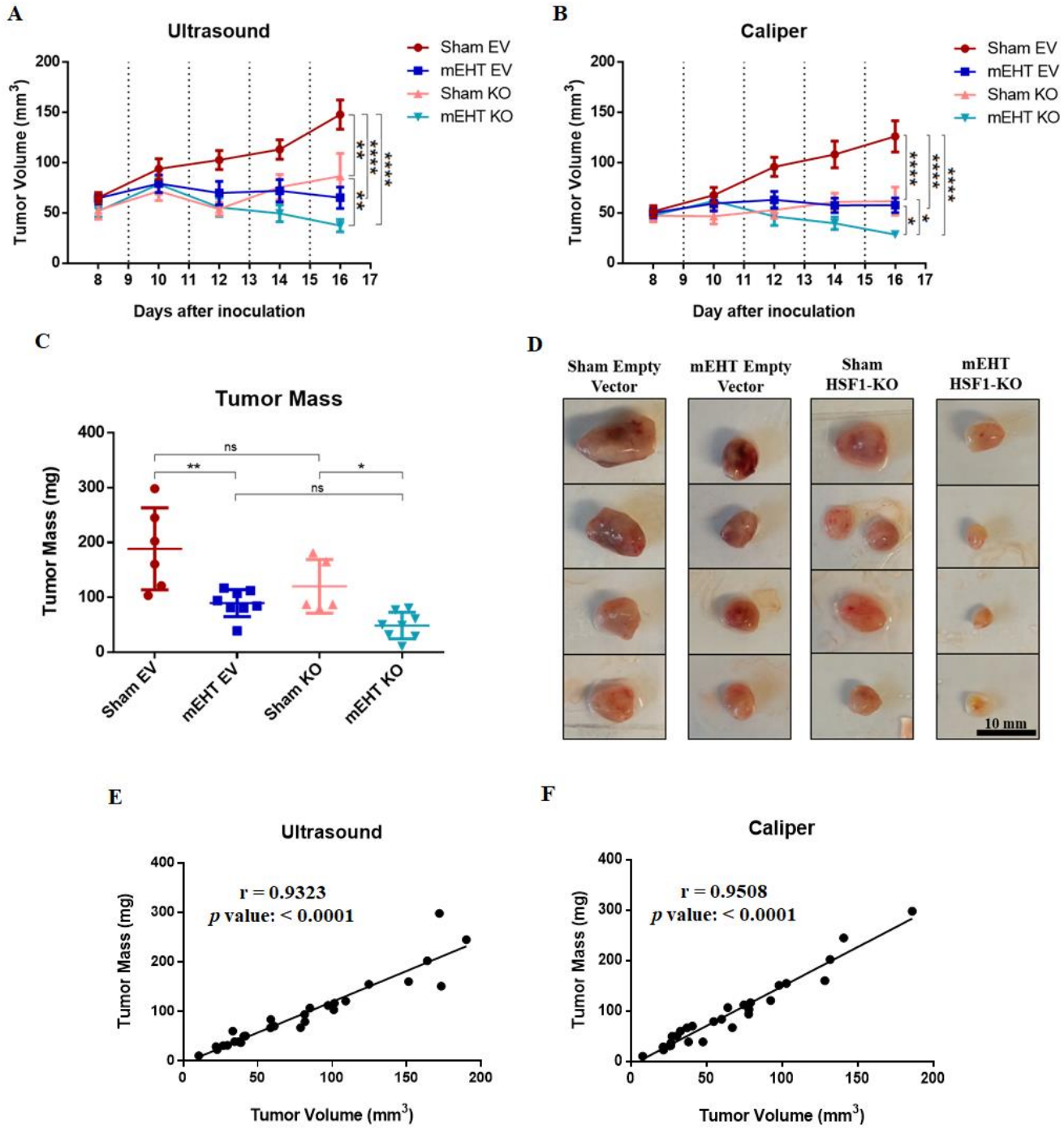

Figure 11. Tumor volume time-course and tumor mass at study termination after 4 mEHT treatements. Tumor growth inhibition as measured by **A)** ultrasound and **B)** digital caliper; **C)** Tumor mass and **D)** four representative tumor images of each group (columns) by experiment termination. Correlation between tumor mass and tumor volume by **E)** US **F)** caliper. Mean ± SD, One-way and Two-way ANOVA, Mean ± SD, n = 6-8/group, ns = not significant, * $p < 0.05$, ** $p < 0.01$, *** $p < 0.001$, **** $p < 0.0001$. Published by Viana *et al.* (176).

4.4. mEHT-induced tumor destruction was enhanced in HSF1-KO tumors

The area of tumor destruction, quantified as the tumor destruction ratio (TDR), was consistently minimal in all sham tumors, regardless of whether they were EV or KO transfected (**Figure 12A** - red marked area). In contrast, mEHT-treated tumors exhibited a substantial increase in tissue damage compared to the sham group (**Figure 12A, B**). Notably, the severe tumor damage induced by mEHT was further increased in the mEHT-treated HSF1-KO group (mEHT EV: 74.6 ± 11%; mEHT HSF1-KO: 84.1 ± 10.6%, p = 0.52, ns). It is important to mention that histopathological data is unavailable for one sham KO and one mEHT KO sample due to their small tumor size.

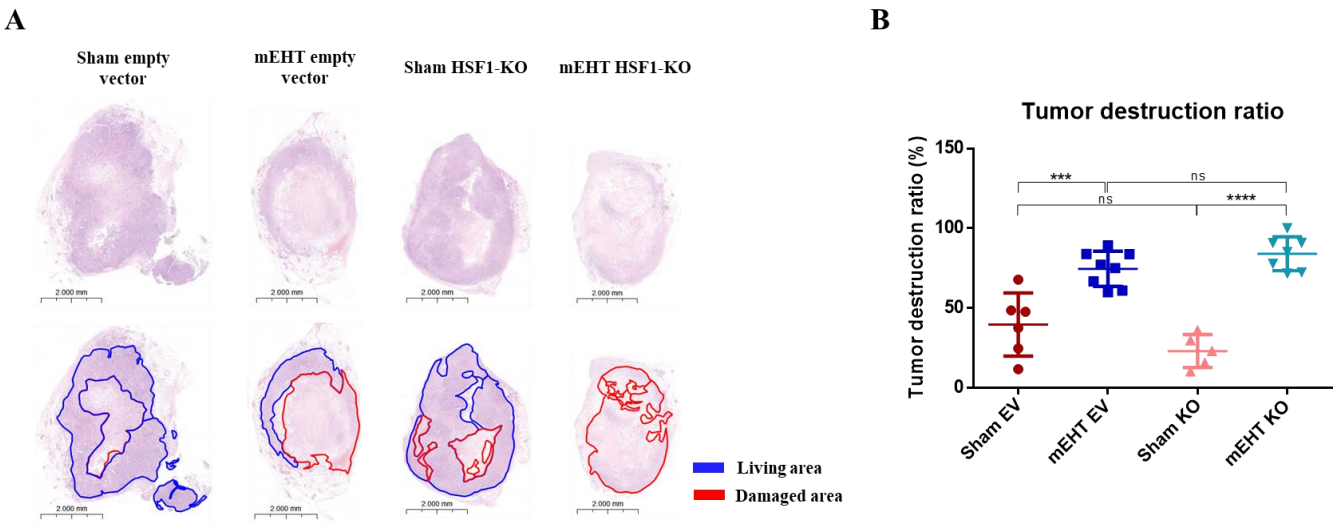

Figure 12. Tumor destruction ratio (TDR) after 4 mEHT treatments. A) Representative tumor images (H&E, 1.0x); **B)** Quantification of TDR on H&E-stained tumors. One-way ANOVA test, Mean ± SD, n = 5-8/group, ns = not significant, *** $p < 0.001$, **** $p < 0.0001$. Published by Viana *et al.* (176).

4.5. HSF1-KO prevented HSF1 and HSP70 upregulation after mEHT treatment *in vivo*

Relative HSF1 mRNA level, as assessed after four sham or mEHT treatments in EV-treated tumors, was significantly reduced in the KO groups, demonstrating effective silencing (**Figure 13A**). HSF1 mRNA was not

significantly influenced by mEHT in the knockdown group. On the other hand, mEHT significantly increased HSF1 in the empty vector group. The relative HSP70 mRNA level, as assessed after four sham treatments, increased in mEHT-treated groups (**Figure 13B**). As expected, mEHT stimulated HSP70 mRNA significantly only in the EV-treated tumors. mEHT did not induce a significant HSP70 response in HSF1-KO mEHT tumors.

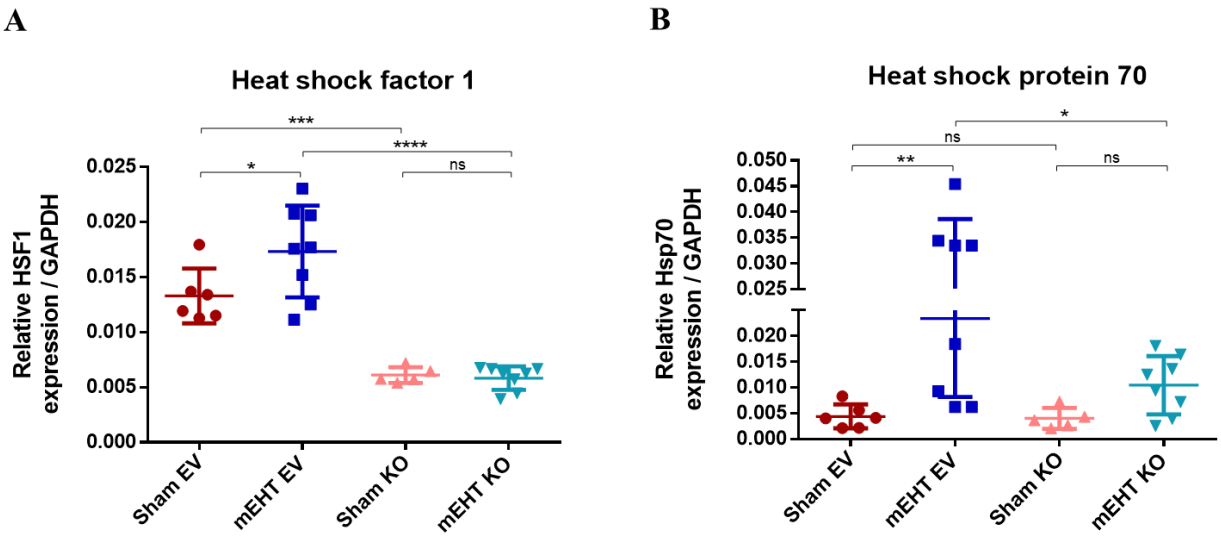

Figure 13. HSF1 and HSP70 mRNA relative expression after 4 mEHT treatments. A) HSF1; **B)** HSP70. GAPDH: Glyceraldehyde 3-phosphate dehydrogenase: housekeeping gene. One-way ANOVA, Mean ± SD, n = 6-8/group, ns = not significant, * $p < 0.05$, ** $p < 0.01$, *** $p < 0.001$, **** $p < 0.0001$. Published by Viana *et al.* (176).

Immunohistochemistry (IHC) staining specific for HSF1 was present in most nuclei of empty vector treated tumors (**Figure 14A, B** - upper row). Such specific HSF1 staining was not identified in HSF1-KO tumors (**Figure 14A, B** - lower row). HSF1 protein expression was not influenced by mEHT (**Figure 14A, B** - right column).

HSP70 specific protein staining was intense cytoplasmic staining in mEHT treated tumors. Such specific staining was absent in sham treated tumors (**Figure 14C, D** - left column), demonstrating only background staining. Four mEHT treatments induced significant upregulation of HSP70, marked with intense specific staining in mEHT-treated EV tumors (**Figure 14C, D**). Such HSP70 induction was not significant in the mEHT KO group *vs* sham KO

demonstrating that HSF1-KO was able to reduce the mEHT induced HSP70 expression. HSP70 induction was significantly inhibited in the KO *vs* EV mEHT-treated groups (**Figure 14C**).

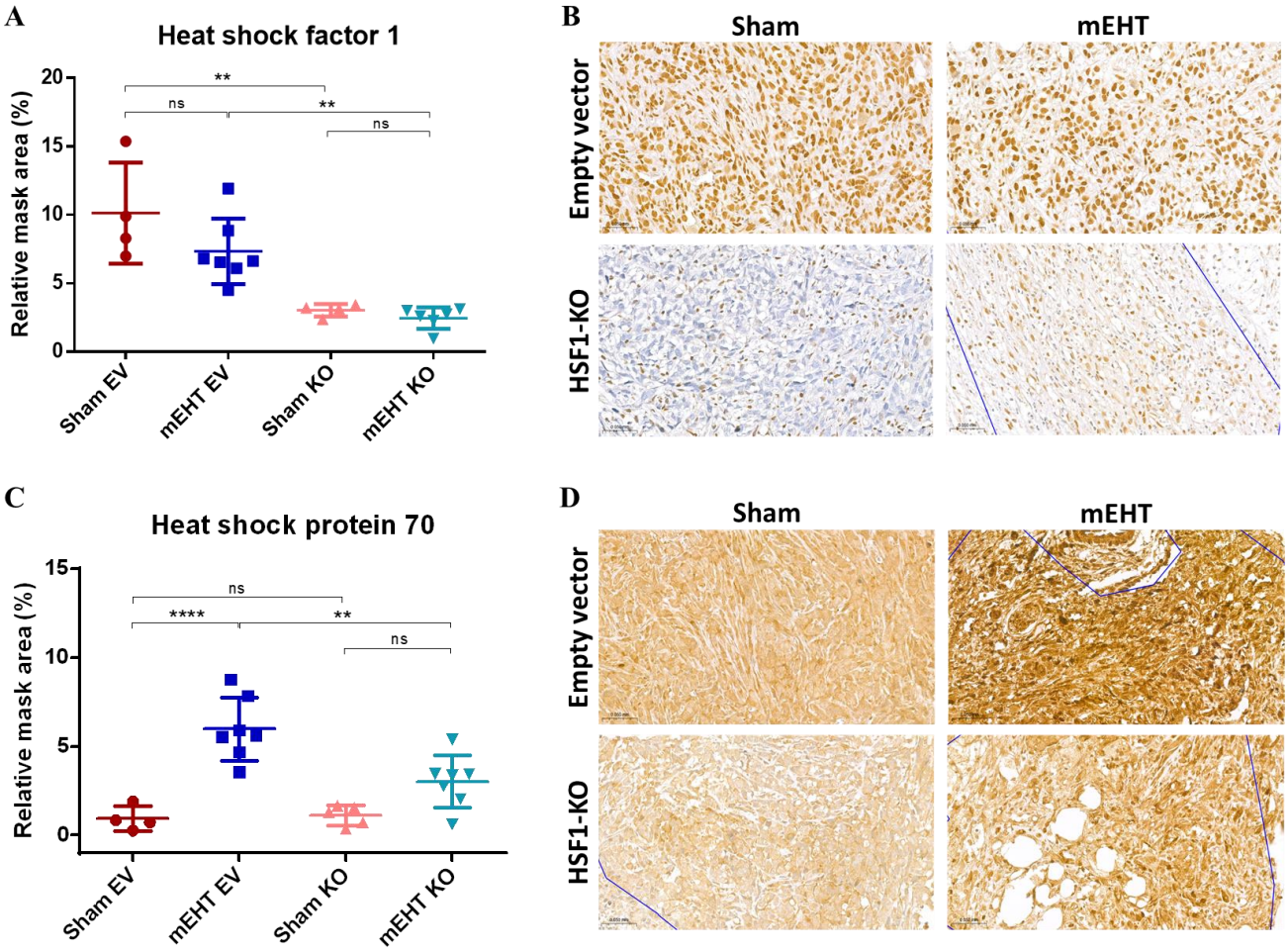

Figure 14. HSF1 and HSP70 protein detection and quantification with immunohistochemistry after 4 mEHT treatments. A) HSF1 and **C)** HSP70 protein quantification, and representative sections of **B)** HSF1 and **D)** HSP70, 40x magnification. One-way ANOVA, Mean ± SD, n = 4-7/group, ns = not significant, * $p < 0.05$, ** $p < 0.01$, *** $p < 0.001$. Published by Viana *et al.* (176).

4.6. mEHT-tumor growth reduction was synergistically enhanced by the heat shock inhibitor, KRIBB11, after 4 mEHT treatments

The volume of Sham + Veh (vehicle) 4T1 wild type tumors increased almost 4-times during the experiment (**Figure 15A, B** - red). KRIBB11 monotherapy did not influence tumor growth significantly (rose). However,

mEHT treated tumors grew slower (dark blue) and their size was significantly reduced after the 4th treatment. Tumor growth rate was further reduced significantly in the KRIBB11 + mEHT co-treated group (light blue) as measured by ultrasound and caliper. Despite similar tumor volumes at the beginning of the treatments, mEHT tumors were significantly smaller than sham tumors at the end of the study. Supporting tumor volume data, tumor mass was reduced only by mEHT but not by KRIBB11 alone. The tumors were significantly the smallest in the KRIBB11 + mEHT co-treated group (**Figure 15C, D**) by study termination. Demonstrating the reliability of tumor volume measurements during follow-up, tumor volume strongly correlated with tumor mass (**Figure 15E, F**).

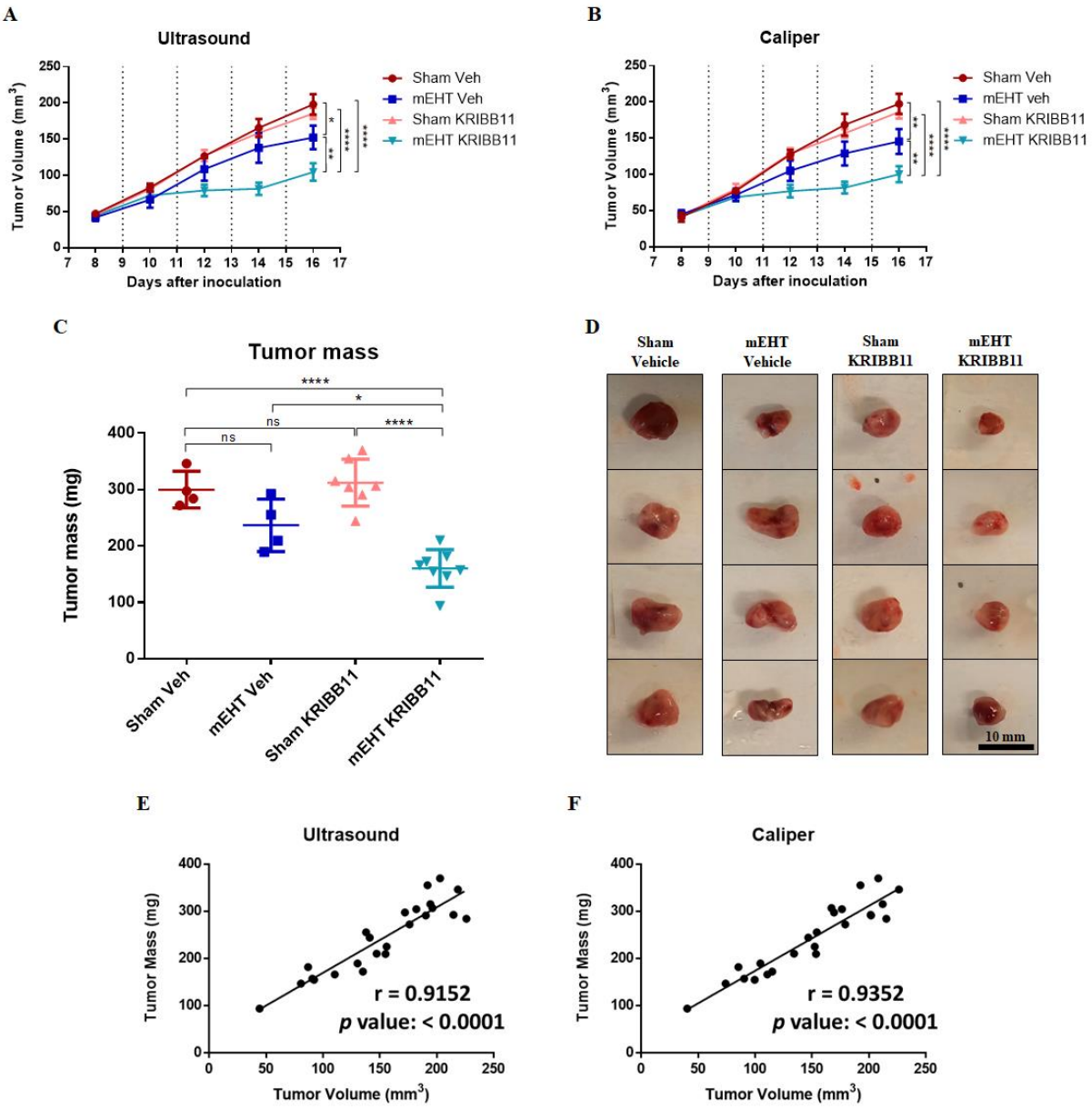

Figure 15. Time-course of tumor volume and tumor mass in 4T1 Wild Type (WT) cells at study termination following combination therapy experiment. Tumor growth inhibition as measured by **A)** ultrasound and **B)** digital caliper. **C)** Tumor mass and **D)** four representative tumor images of each group (columns) by experiment termination. Correlation between tumor mass and tumor volume by **E)** US and **F)** caliper. Mean ± SD, One-way and Two-way ANOVA, Mean ± SD, n = 4-8/group, ns = not significant, * $p < 0.05$, ** $p < 0.01$, **** $p < 0.0001$. Published by Viana *et al.* (176).

4.7. KRIBB11 prevented HSP70 upregulation after 4 mEHT treatments

Relative HSF1 mRNA level as assessed after four sham or mEHT treatments was reduced in the KRIBB11 treated groups demonstrating effective inhibition of the heat shock response in treated tumors (**Figure 16A**). HSF1 mRNA was not influenced significantly by mEHT.

Relative HSP70 mRNA level was assessed after four treatments. Although mEHT induced an increase in HSP70 mRNA compared to the sham group, this difference did not reach statistical significance (**Figure 16B**). In contrast, HSP70 elevation was absent in KRIBB11 treated tumors receiving mEHT, and HSP70 mRNA levels were significantly lower in the mEHT + KRIBB11 group compared to the mEHT + Veh group.

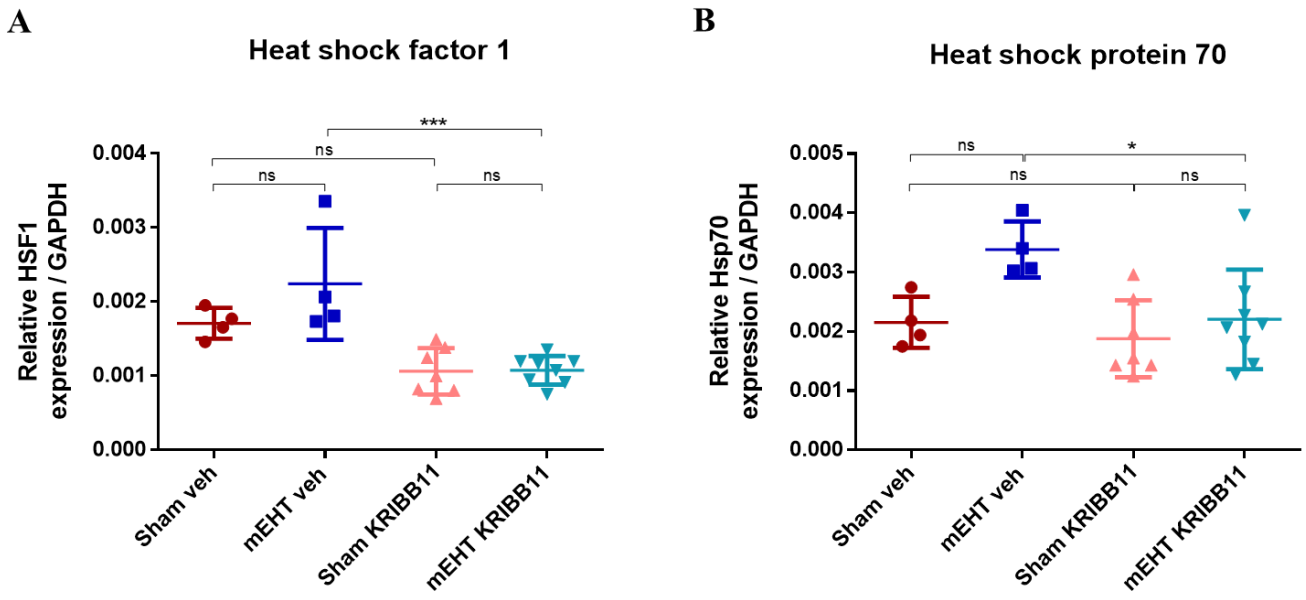

Figure 16. HSF1 and HSP70 mRNA relative expression after 4 mEHT *in vivo* treatments in 4T1 Wild Type (WT) tumors. A) HSF1. **B)** HSP70. GAPDH: Glyceraldehyde 3-phosphate dehydrogenase: housekeeping gene. One-way ANOVA, Mean ± SD, n = 4-8/group, ns = not significant, * $p < 0.05$, *** $p < 0.001$. Published by Viana *et al.* (176).

In tumors treated with mEHT + Veh, Immunohistochemistry (IHC) staining specific for HSF1 displayed prominent nuclear staining (**Figure 17A, B** – upper right panel). In contrast, KRIBB11 did not significantly reduce HSF1

expression, as the levels of KRIBB11-treated groups were comparable to sham vehicle (**Figure 17A, B** – lower panel). Interestingly, the combination treatment of KRIBB11 and mEHT demonstrated a synergistic effect, as seen by the significant lack of upregulation in HSF1 expression compared to the KRIBB11 + Vehicle group (**Figure 17A**).

Intense cytoplasmic staining specific to HSP70 protein was observed exclusively in tumors treated with mEHT monotherapy (**Figure 17C, D** – right columns). In contrast, such distinctive staining was notably absent in sham treated tumors, indicating only background levels of HSP70 (**Figure 17C, D** – left columns). The mEHT-induced upregulation of HSP70 was significantly attenuated by co-treatment with KRIBB11, emphasizing the inhibitory effect of HSF1 on mEHT-induced HSP70 expression (**Figure 17C**).

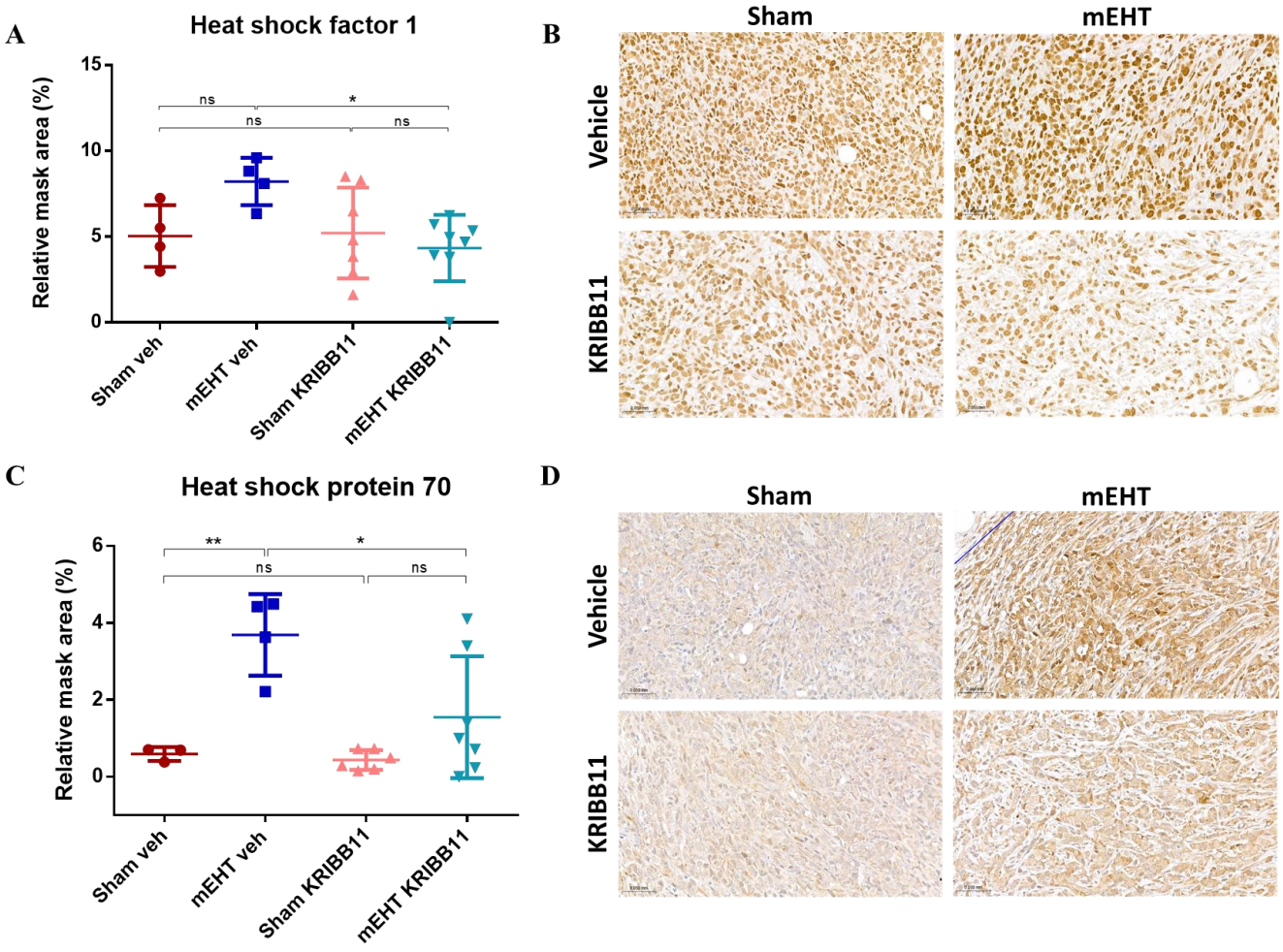

Figure 17. HSF1 and HSP70 protein detection and quantification with immunohistochemistry after 4 *in vivo* mEHT treatments in 4T1 Wild Type (WT) tumors. A) HSF1 and **C)** HSP70 protein quantification. Representative sections of **B)** HSF1 and **D)** HSP70, 40x magnification. One-way ANOVA, Mean ± SD, n = 3-8/group, ns = not significant, * $p < 0.05$, ** $p < 0.01$. Published by Viana *et al.* (176).

4.8. Slightly increased tumor destruction tendency was observed in tumors treated with combined therapy

Tumor Destruction Ratio (TDR) revealed significant tissue damage in mEHT + KRIBB11-treated samples compared to sham (**Figure 18A**, **B**). The image below shows that the core damaged area in cancers varies with tumor mass, resulting in a moderate negative correlation between TDR and tumor mass ($r = -0.5383$, $p = 0.0098$) (**Figure 18B**). In general, sham groups (Vehicle and KRIBB11) were larger in size and had moderate TDRs. However, three samples deviated from this trend, one in Sham + Vehicle (61.05%) and two in Sham + KRIBB11 groups (67.39% and 70.49%), all other sham tumors displayed TDR < 55% (**Figure 18**). Nonetheless, the mEHT-treated groups (Vehicle or KRIBB11) were smaller and exhibited larger TDRs. With only two exceptions, both in the mEHT + KRIBB11 group (49.22% and 51.39%), all cancers demonstrated TDRs over 70% (**Figure 18B**).

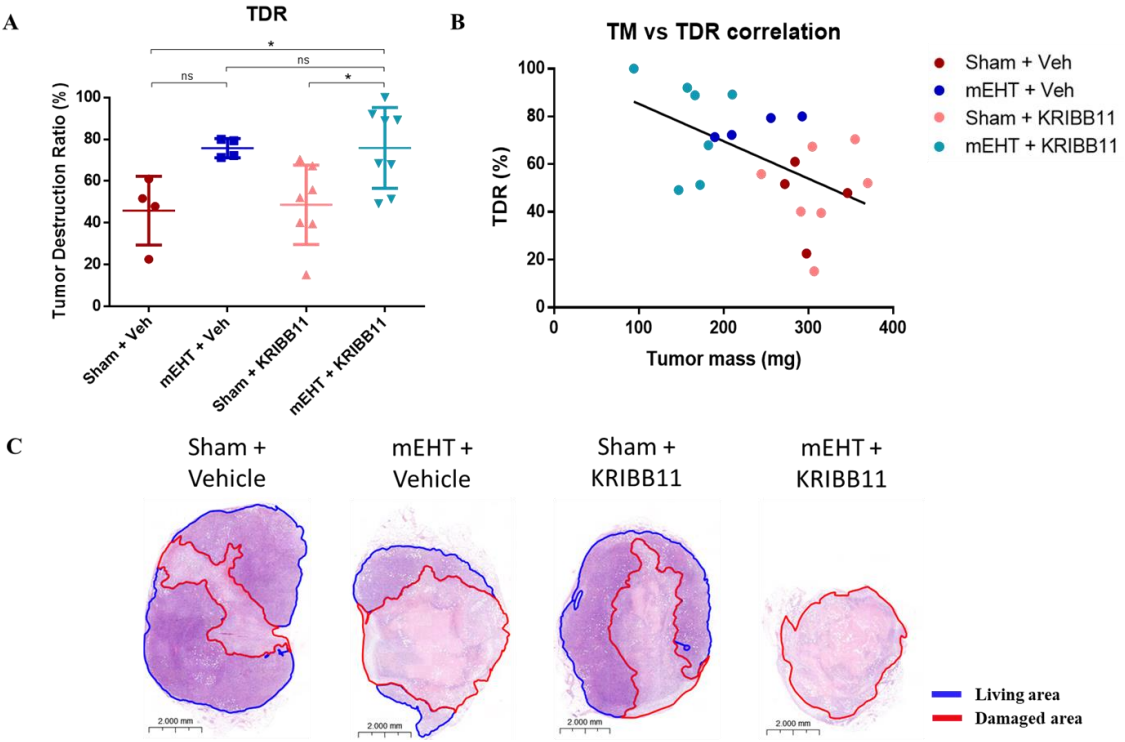

Figure 18. Effects of combined therapy (mEHT + KRIBB11) on Tumor Destruction Ratio (TDR) in 4T1 Wild Type (WT) cells. A) Quantification of TDR on H&E-stained cancers. **B)** Scatter diagram and linear regression line showing the relationship between TDR (Y axis) and tumor mass (X axis), which reveals a negative correlation between TDR and tumor mass (TDR, cancer destruction ratio). **C)** Representative tumor images (H&E, 1.0x). One-way ANOVA test, Mean ± SD, n = 4-8/group, ns = not significant, * $p < 0.05$. Published by Viana *et al.* (176).

4.9. Analysis of mEHT effects on gene expression revealed upregulation of progesterone receptor expression

Next-generation sequencing of RNA (NGS RNA-Seq) was conducted on 4T1 TNBC tumor samples collected 24 hours after the last mEHT treatment to explore gene expression changes induced by mEHT. Among the 290 Differently Expressed (DE) genes (criteria: $p < 0.05$ or log10(p) < 1.30103; Fold Change (FC) > 2 or logFC > 1), progesterone receptor (PGR) demonstrated significant upregulation in the mEHT-treated group (FC = 16.05; p value = 0.01) in our TNBC mouse model (**Table 3** and **Figure 19A**). A Volcano plot visualization of gene logFC and –log10(p) values of NGS data is presented in **Figure 19B**, where PGR is highlighted as a red dot.

Table 3. Next-Generation Sequencing (NGS) identified progesterone receptor among the top 10 differently expressed genes

Next-generation sequencing data			
Description	**geneName**	**FC**	**P.Value**
inter-alpha trypsin inhibitor, heavy chain 2	Itih2	31.07692	2.07E-05
fibrinogen beta chain	Fgb	28.35026	0.000206
inter alpha-trypsin inhibitor, heavy chain 4	Itih4	22.72484	0.000267
CD5 antigen-like	Cd5l	19.61978	0.162018
casein kappa	Csn3	19.42657	0.004284
aldehyde dehydrogenase family 1, subfamily A7	Aldh1a7	18.06375	0.000925
klotho beta	Klb	17.67851	0.001533
carbonic anhydrase 3	Car3	16.85459	0.000349
progesterone receptor	**Pgr**	**16.05732**	**0.014099**
neuronatin	Nnat	15.83486	0.002261

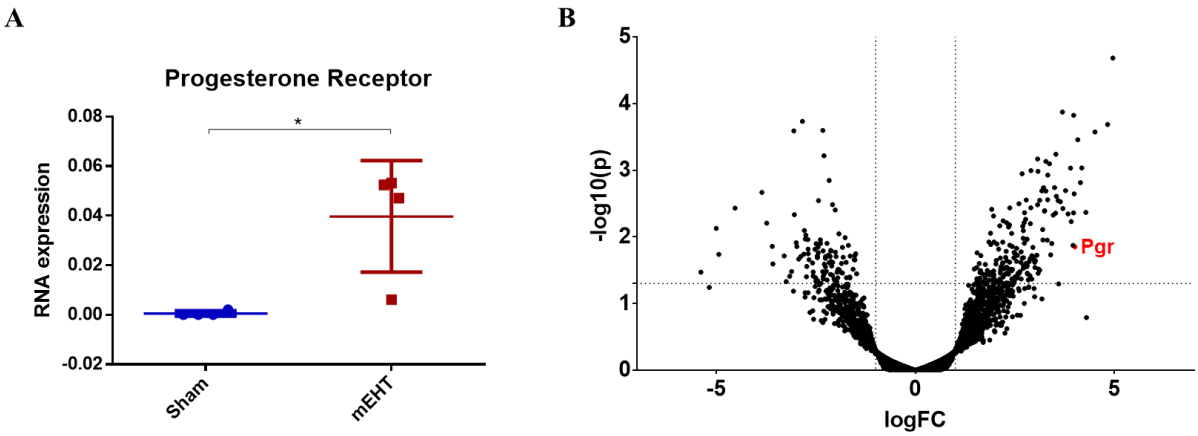

Figure 19. Multiplex analysis of Progesterone Receptor (PGR) re-expression in 4T1 Wild Type (WT) Triple-Negative Breast Cancer (TNBC) mouse model following mEHT treatments. A) Next-generation sequencing (NGS) revealed upregulation of PGR in the mEHT group. **B)** Volcano plot visualization of all genes according to NGS RNA Seq data. −log10(p) values plotted against fold changes (logFC). Vertical dotted line: logFC = 1, horizontal dotted line: −log10(p) = 1.30103. PGR is highlighted in red. Statistical analysis performed using t-test, Mean ± SD, n = 4/group, * $p < 0.05$. Published by Schvarcz *at al.* (89).

For validation of gene expression at the mRNA level, individual mRNA molecular counting was performed with NanoString nCounter® Technology (NanoString Technologies, Seattle, WA, USA). One hundred and thirty-four DE target genes from NGS data were sorted to create a custom NanoString panel. Again, among the 134 target genes identified by NanoString, PGR was significantly upregulated (p value = 0.0094) in the mEHT-treated group

(**Figure 20A**). The detailed NGS and NanoString data was published by our group (89). PGR mRNA levels were further analyzed by RT-PCR. Compared to sham group, the mRNA expression of PGR gene was significantly upregulated (*p* value = 0.0056) after mEHT treatments (**Figure 20B**). The same significant trend was observed in the overall sample analysis for this *in vivo* experiment (sham: 10; mEHT: 11) assessed by qPCR (**Figure 20C**). Taken together, the multiplex analysis and qPCR demonstrated re-expression of PGR by mEHT in 4T1 TNBC cell line.

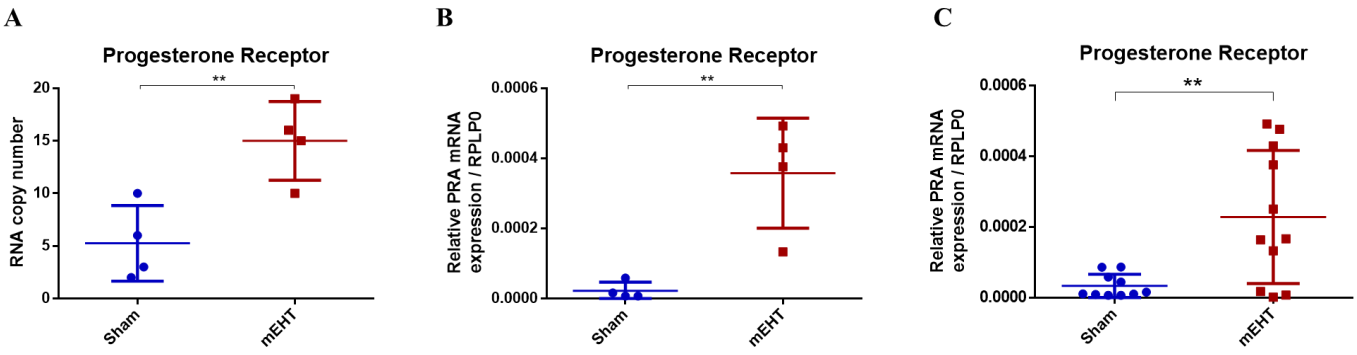

Figure 20. Multiplex analysis and RT-PCR of Progesterone Receptor (PGR) re-expression in 4T1 Wild Type (WT) Triple-Negative Breast Cancer (TNBC) mouse model following mEHT treatments. A) NanoString analysis and **B**) RT-PCR further confirmed the re-expression of PGR in 4T1 TNBC cell line. **C)** RT-PCR collection data of all samples used in this mEHT *in vivo* experiment. Statistical analysis performed using t-test, Mean ± SD, n = 4/group, ** $p < 0.01$. Unpublished data.

4.10. mEHT upregulated PGR protein expression in TNBC malignant tumors

To confirm the re-expression of PGR by mEHT treatments *in vivo*, PGR expression was assessed through immunohistochemistry (IHC) (**Figure 21**). Consistent with the multiplex analysis and qPCR, the percentage of relative PGR masked area significantly increased in mEHT-treated malignant tumor samples (3.533 ± 0.4817%) compared to sham group (1.723 ± 0.4295%) (*p* value = 0.031). **Figure 21B** shows representative tumor images illustrating the intensity of PGR staining in sham and mEHT-treated samples.

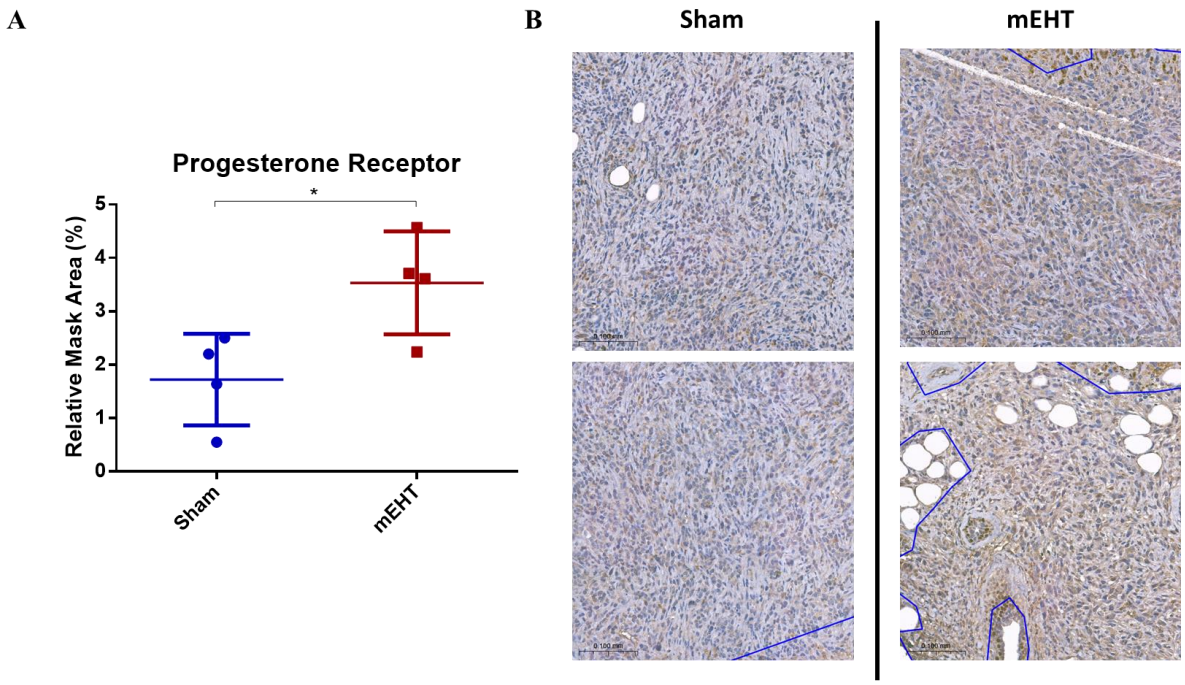

Figure 21. Effect of modulated electro-hyperthermia (mEHT) treatments on the re-expression of Progesterone Receptor (PGR) protein in 4T1 Wild Type (WT) Triple-Negative Breast Cancer (TNBC) cell line. A) Quantification of PGR protein by immunohistochemistry (IHC) demonstrated significant upregulation in the mEHT group. **B**) Representative tumors from sham and mEHT-treated mice with PGR staining, 40x magnification. Statistical analysis performed using t-test, Mean ± SD, n = 4/group, * $p < 0.05$. Unpublished data.

4.11. Increased sensitivity to mifepristone and ulipristal acetate in combination with mEHT in TNBC cells

To establish a model for investigating the mechanisms underlying PGR re-expression through mEHT treatment in a TNBC cell line and its potential synergy with selective progesterone receptor modulators (SPRMs), 4T1 cells were chronically exposed to increasing concentrations of mifepristone (MIF) or ulipristal acetate (UPA) *in vitro*. An analysis of the resazurin assay data with the increasing concentration of SPRMs demonstrated a dose-dependent decrease in number of viable cells. The growth inhibitory potency of both antiprogestins, MIF and UPA, represented by the half maximal inhibitory concentration (IC_{50}) values, is summarized in **Table 4**. MIF exhibited an IC_{50} of 32.76 µM, while UPA had an IC_{50} of 34.35 µM. However, dose-response

curves (**Figure 22A**) indicated that complete cell death was not observed in cell cultures treated with either SPRM up to 40 μM.

Table 4. Concentration of mifepristone and ulipristal acetate needed to achieve 50% growth inhibition of 4T1 triple-negative breast cancer cell line

Selective Progesterone Receptor Modulator	IC50 (μM)
Mifepristone	32.76 ± 1.605
Ulipristal Acetate	34.35 ± 2.28

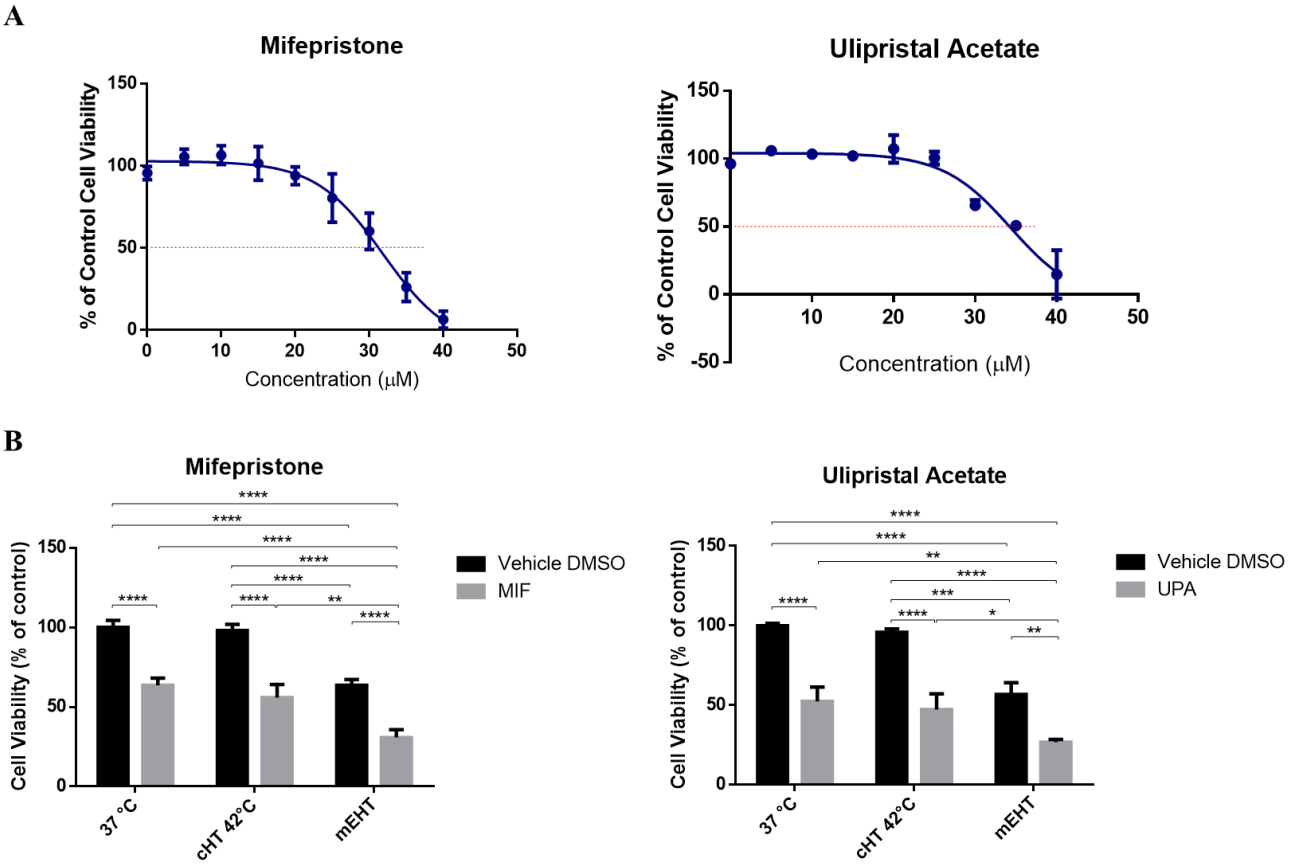

Figure 22. Inhibition of cell growth by Selective Srogesterone Receptor Modulators (SPRMs), Mifepristone (MIF) and Ulipristal Acetate (UPA) in 4T1 Wild Type (WT) Triple-Negative Breast Cancer (TNBC) cell line. A) Dose-response curves showing the effects of MIF and UPA at different concentrations on cell viability measured by the resazurin assay. The dashed red lines show the IC_{50} for each SPRM. **B**) The impact of conventional hyperthermia (cHT) and modulated electro-hyperthermia (mEHT) in combination with MIF and UPA on cell viability, demonstrating synergism with the combination of mEHT and the antiprogestins, as evidenced by significant reduction in cell viability. Statistical analysis performed using **A**) nonlinear regression (GraphPad Prism) and **B**) Two-way ANOVA, Mean ± SD, n = 4/group, * $p < 0.05$, ** $p < 0.01$, *** $p < 0.001$, **** $p < 0.0001$. Unpublished data.

In our study, the murine 4T1 TNBC cell line synergistically responded to MIF and UPA when treated with mEHT *in vitro* (**Figure. 22B**). The results demonstrated significant decrease in cell viability up to 63.67% and 52.45% due to MIF and UPA, respectively, which was further enhanced to 30.8% and 26.85% when MIF and UPA was applied with mEHT, respectively. However, combined therapy using SPRMs and conventional hyperthermia (cHT) did not yield a statistically significant difference compared to the effect observed with MIF and UPA alone (*p* values = 0.7719 and 0.9981, respectively, ns). These results indicate that mEHT synergizes with SPRMs, while cHT does not synergize at the same temperature and duration of time.

5. Discussion

Modulated electro-hyperthermia (mEHT) is a loco-regional non-invasive cancer therapy which has been successfully applied *in vitro*, *in vivo*, and in the clinics for over 30 years (95). The mEHT treatment triggers apoptosis and necrosis of cancer cells via thermal and non-thermal effects such as membrane perturbations (similarly to electrophoresis), and the radiofrequency field also induces temperature increase to 42°C (101). The high energy absorbed by cancer cells and specifically cancer cell membranes lipid rafts consequently disrupts membrane arrangement and integrity on the basis of its elevated oxidative glycolysis (Warburg effect), ion concentration, and conductivity compared to adjacent normal tissues (120), therefore inducing anti-cancer response (105). However, it is known that mEHT provokes cell- and heat-stress throughout the increase of extracellular heat shock protein 70 (HSP70) release (106). In our previous studies, we demonstrated that mEHT induced a robust heat shock response in our mouse cancer model, resulting in strong upregulation of HSP70 (90). It is worth noting that HSP70, a crucial molecular chaperone, typically maintains low or undetectable levels in unstressed cells (107). The transcription of HSP70 is triggered by Heat Shock Factor 1 (HSF1), a master regulator of the heat shock response (18). It has been demonstrated in a wide range of cancer types that HSF1 has a cytoprotective activity and supports cancer cell proliferation, survival, invasion, and metastasis (146). Targeting HSF1 in cancer therapy has been suggested before (154), and carcinogenesis was inhibited in HSF1-knockdown experiments in mammary (37), liver (178), and skin (31) cancer models. We therefore hypothesized that the inhibition of Heat Shock Response (HSR) by inhibiting HSF1 would enhance the therapeutic potential of mEHT. As a proof-of-concept, we used genome editing tools to knockdown HSF1. To investigate the translational potential, we also studied a small molecule inhibitor (KRIBB11), aiming to inhibit HSF1 and thus enhance the anticancer effects of mEHT treatment.

In the present study, CRISPR/Cas9-mediated HSF1 knockdown was successful in 4T1 murine breast cancer cells. While the use of CRISPR to completely ablate genes can be challenging, as this system rarely eliminates the

expression of a target gene entirely, leading to low knockdown efficiencies (< 80%) (179, 180), we achieved an impressive knockdown efficacy of over 95% (**Figure 9**). This high efficacy was evidenced by the GFP-positivity of transduced cells after antibiotic selection (puromycin) and FACS sorting. However, these strategies seemed to be less effective in the empty vector group (62.83%). This group used a non-targeting guide RNA with no specific target site on the entire genome, designed to serve as a control group with a wild type phenotype. The genome editing using the CRISPR/Cas9 lentiviral empty vector did not enable gene truncation via real time polymerase chain reaction (PCR) (**Figure 10**). On the other hand, we achieved a very strong HSF1 knockdown efficiency as demonstrated by flow cytometry and confirmed by real-time PCR (**Figure 13**). Immunohistochemistry analysis of *in vivo* malignant tumors further corroborated the HSF1 knockdown (**Figure 14**). HSF1 expression was reduced and hyperthermia-induced HSP70 upregulation was inhibited in HSF1-KO cells.

mEHT cancer selectivity and its inhibition of tumor growth have been reported in a wide range of cancer types (96). Previously we also demonstrated inhibition of tumor growth by mEHT monotherapy in our murine breast cancer model (89, 90). In this study, we observed a significant enhancement in tumor growth inhibition with mEHT treatment in HSF1-KO cells. HSF1-KO malignant tumors exhibited a size reduction of over 50% compared to non-mEHT-treated empty vector tumors (**Figure 11**). This aligns with previous findings suggesting the essential role of the HSF1 gene in cancer development, as HSF1-KO tumors naturally grow at a slower rate than empty vector tumors (181). mEHT further amplified the reduction in tumor growth in the KO group. Therefore, the importance of HSF1 supporting tumor progression can be demonstrated by the susceptibility reduction of HSF1-KO cells to cancer formation (74).

Besides tumor size reduction, tumor destruction, damaged pale areas which are assessed based on Tumor Destruction Ratio (TDR), was enhanced in mEHT-treated HSF1-KO samples (**Figure 12**), suggesting that the protective mechanisms from HSPs had been exhausted by the HSF1 knockdown construct

(131). On another hand, we observed a discrete non-significant elevation of HSP70 mRNA in the knockdown group treated with mEHT (**Figure 13**). This result corresponds with the fact that HSP70 may also be expressed regardless HSF1 transcriptional activity, and other factors such as different cellular signaling pathways might also regulate HSP70 status and activity (182, 183).

Based on our previous data (90) and the present HSF1 knockdown study, we hypothesized that the inhibition of HSR by KRIBB11, a specific inhibitor of HSF1, could potentiate the anticancer effects of mEHT in tumor allografts. Mouse xenograft cancer studies have demonstrated reduction of tumor growth in samples treated daily with KRIBB11 dose in human colon- (148), breast- (150), bladder- (153), and liver cancers (184), both alone or in combination with other chemical compounds. When in combination, KRIBB11 efficacy was increased (150, 151). Here, we established the synergism between four-mEHT treatments and daily dose of KRIBB11 at 50 mg/Kg for 8 days, as demonstrated by tumor volume and tumor mass reduction in the combined therapy group (**Figure 15**). However, KRIBB11 was not able to reduce tumor mass in monotherapy (**Figure 15C**). Carpenter *et al.* reported similar findings, stating that KRIBB11 did not significantly inhibit tumor growth in a breast cancer model unless combined with an AKT inhibitor (150). In another study a dose of 50 mg/Kg of KRIBB11 did not reduce myeloma xenograft growth, whereas a dose of 65 mg/Kg proved effective (156).

The effects of KRIBB11 abovementioned were achieved by following the protocol established by Yoon *et al.*, which involved daily administration of KRIBB11 over a period of 18 days (148). However, due to our experiment's shorter duration (8 days), our mice received fewer KRIBB11 injections. This decision was based on our findings, which demonstrated that prolonged mEHT treatments could lead to substantial damage in tumor tissue. This damage hinders the isolation and detection of RNA from treated malignant tumors, thereby impeding molecular analysis (89). This may also account for the observed lack of significant tumor growth inhibition with KRIBB11 monotherapy.

While previous studies have demonstrated that mEHT induces the heat shock response mainly by upregulation of HSPs (89, 90, 105, 106), we observed that mEHT may not directly lead to significant changes in HSF1 mRNA (**Figure 16**) and protein levels (**Figure 17**). Instead, the regulation of HSF1 might primarily occur through its cellular localization, particularly its movement from the cytoplasm to the nucleus in response to stress (185). This nuclear translocation of HSF1 is a crucial step in initiating the transcription of additional HSPs.

Aligned with the HSF1-KO TDR data, the damaged area observed in the combined mEHT and KRIBB11 therapy did not show statistically significant differences compared to mEHT + vehicle (**Figure 18**). While tumor volume and mass reduction demonstrated synergistic enhancement of the mEHT effect with additional KRIBB11 therapy, the TDR results were not as pronounced. This could be attributed to the extensive destruction observed in sham tumors, as noted by our group (89). The elevated mitochondrial metabolism of 4T1 cancer cells might contribute to necrosis development as a result of low oxygen levels and nutrient supply (186). Therefore, the damage magnitude may be related to tumor size (187). Indeed, our study revealed that larger tumors tended to have moderate TDR's (**Figure 18b**). This trend was primarily due to their large size, with most of them belonging to the sham groups (vehicle and KRIBB11). Consequently, the necrosis observed at the core of sham tumors was a direct result of cancer outgrowth (**Figure 18b**, red and pink dots). In contrast, mEHT-treated tumors exhibited a notably high TDR along with reduced mass (**Figure 18b**, dark blue and green dots). From this, we infer that necrosis observed in mEHT groups (both vehicle and KRIBB11) arose from the cancer-killing effect of mEHT. Furthermore, this effect was amplified by administration of KRIBB11 (**Figure 18b**, green dots). This suggests that the increase in cancer core destruction in sham groups is primarily linked to tumor size, whereas in mEHT groups, it is more likely due to the treatment itself.

In conclusion, we have demonstrated that the combination of modulated electro-hyperthermia (mEHT) with the CRISPR/Cas9 gene-editing technique significantly enhances its anticancer effects *in vivo*. Specifically, the

knockdown of heat shock transcription factor 1 (HSF1) led to the inhibition of tumor growth and a reduction in HSP70 upregulation induced by mEHT. Moreover, the administration of the specific heat shock inhibitor, KRIBB11, amplified the therapeutic impact of mEHT. These findings suggest a potential synergy between KRIBB11 and established clinical anticancer therapies like mEHT. Consequently, KRIBB11 holds promise for translation into clinical applications, offering a potentially impactful addition to cancer treatment modalities.

The reactivation of the progesterone receptor (PGR) in the triple-negative breast cancer 4T1 cell line was another topic addressed in the present study. On this study conducted by our group, employing next-generation sequencing (NGS), we identified 290 genes that were differently expressed (DE), either upregulated or downregulated, following mEHT treatments in a TNBC mouse model (89). Notably, PGR ranked among the top 10 differently expressed genes, exhibiting a significant upregulation with a fold-change of 16.05 and a *p* value 0.01 compared to sham group (**Figure 19**). Interestingly, despite our findings, a recent multi-omics characterization of the 4T1 cells reported no expression of PGR (188). Our group decided to investigate the molecular effects of mEHT on the potential re-expression of PGR in 4T1 TNBC cells, based on these findings. We expanded the findings in our multiplex analysis by conducting a more comprehensive investigation at the RNA level using NanoString and RT-qPCR, specifically targeting the PGR gene. Our results indicate a significant upregulation of PGR expression level following mEHT treatments (*p* value = 0.0094) compared to the sham group by NanoString (**Figure 20A**). Consistent with NGS and NanoString findings, RT-qPCR also demonstrated a significant upregulation of PGR in the mEHT group (*p* value = 0.0056) (**Figure 20B**). While NGS and NanoString analyses were limited to 8 malignant tumor samples, qPCR included all 21 samples from the experiment. Despite the difference in sample size, the mEHT group exhibited a consistent significant upregulation trend in PGR expression (*p* value = 0.0045) (**Figure 20C**).

The presence of PGR was also checked in the protein level by immunohistochemistry (IHC). The relative masked area (rMA), representing the ratio of PGR expression to the non-damaged area in the tumor sample, exhibited a significant increase in PGR levels in the mEHT group (*p* value = 0.031) (**Figure 21A and B**). Interestingly, TNBC tumors lack immunohistochemical expression of PGR, among other markers (3). This finding, in contrast to Schrörs *et al.* (188), suggest a lower level of PGR expression in non-treated TNBC sham tumors. The variations in PGR expression patterns may be attributed to differences in culture conditions or methodologies used to assess potential PGR expression.

To assess the functionality of the restored PGR as a potential chemotherapy target, we evaluated the response of TNBC malignant tumors to selective progesterone receptor modulators (SPRMs), including mifepristone (MIF) and ulipristal acetate (UPA). First, a dose-response *in vitro* experiment was conducted, exposing the 4T1 TNBC cell line to increasing concentrations of MIF and UPA, revealing the ability of both antiprogestins to inhibit cell growth (**Figure 22A**). Tieszen *et al.* suggested that while it is commonly assumed that MIF and UPA exert their anti-growth effects as PGR antagonists, TNBC cell lines exhibit relatively low sensitivity to SPRMs, as evidenced by their high IC_{50} values, suggesting that these antiprogestins might operate through alternative mechanisms independent of PGR (189). In fact, in our study, the IC_{50} for MIF and UPA was 32.76 μM and 34.35 μM, respectively. When combined with mEHT, MIF and UPA significantly reduced cell viability, indicating synergism between SPRMs and mEHT treatments (**Figure 22B**). These findings are consistent with those of Wargon *et al.*, where the epigenetic modulator decitabine not only restored the expression of PGR but also enhanced the responsiveness effect of the antiprogestin MIF, both *in vitro* and *in vivo*. This resulted in a reduced cell proliferation effect and decreased tumor growth when used in combination (190).

In conclusion, our data suggest that mEHT treatments effectively induce the re-expression of PGR in the 4T1 murine cell line, which represents a TNBC subtype characterized by the absence of PGR expression (188). Our

comprehensive multiplex analysis, assessing mRNA levels through next-generation sequencing (NGS), NanoString, and quantitative PCR, demonstrated an increase in PGR expression following mEHT treatments. The analysis of PGR protein levels by IHC corroborates our findings. Moreover, combining mEHT with antiprogestins MIF and UPA reduced TNBC cell viability compared to monotherapy, indicating potential re-sensitization to SPRM drugs by mEHT and demonstrating synergism between mEHT treatments and these drugs. On the other hand, we did not observe similar synergistic effects when conventional hyperthermia was combined with antiprogestins. These findings show promising translational potential; however, further experiments are required to validate and fully understand their clinical significance. The re-expression of PGR presents promising therapeutic opportunities for triple-negative breast cancer, potentially leading to the development of novel targeted therapies or combination treatment approaches.

6. Conclusion

In this study, we investigated the combined effects of modulated electro-hyperthermia (mEHT) with HSF1 knockdown (KO) and the specific HSF1 inhibitor, KRIBB11, on inhibiting tumor growth in a Triple-Negative Breast Cancer (TNBC) mouse model. We also investigated the potential re-activation of progesterone receptor (PGR) in the 4T1 TNBC mouse model following mEHT treatments, and whether this re-activation sensitizes TNBC cells to antiprogestins, Mifepristone (MIF) or Ulipristal Acetate (UPA). We can further conclude that:

- CRISPR/Cas9-mediated HSF1 knockdown was successful and exhibited high transfection efficiency in 4T1 murine TNBC cells.
- The mEHT cancer cell-killing effect was enhanced by the knockdown of HSF1.
- Integration of KRIBB11 alongside mEHT demonstrated a synergistic effect with significant reduction of tumor growth.
- HSF1 inhibition, either by CRISPR/Cas9 or KRIBB11, resulted in a diminishment of HSP70 upregulation typically seen after mEHT treatments.
- The multiplex analysis and qPCR revealed the re-establishment of PGR expression in 4T1 TNBC mouse model treated with mEHT.
- The re-expression of PGR was also confirmed in the protein level.
- The combination of mEHT treatments and antiprogestins, MIF or UPA, reduced 4T1 cell viability *in vitro*, resulting in additional cell-killing effect.
- Conventional hyperthermia (cHT) did not enhance the cell-killing effect of MIF or UPA.

7. Summary

Breast cancer stands as one of the most prevalent forms of cancer. Within this category, Triple-Negative Breast Cancer (TNBC) is defined by the lack of estrogen and progesterone receptors, and HER2 expression. TNBC poses a unique clinical challenge due to its aggressive nature and limited treatment options, prompting researchers to focus on innovative therapeutic approaches.

Modulated electro-hyperthermia (mEHT) is an innovative cancer treatment that utilizes targeted heating to selectively eliminate malignant cells. However, mEHT can induce the Heat Shock Response (HSR) in cancer cells, and consequently cancer cells can protect themselves through Heat Shock Proteins (HSPs) from repeated treatments. To enhance the efficacy of mEHT in eliminating cancer cells, we explored inhibiting HSF1, the master regulator of the HSR. This involved targeting HSF1 using gene editing technique or specific inhibitor, KRIBB11, to disrupt the protective mechanism of HSR, thereby enhancing the direct impact of mEHT on cancer cells.

Our experiments demonstrated that combining mEHT with either HSF1 knockdown or KRIBB11 administration had a synergistic effect in inhibiting tumor growth in our TNBC mouse model. Moreover, HSF1 inhibition through these approaches significantly decreased HSP70 upregulation induced by mEHT at both molecular and protein levels.

We also investigated the effects of mEHT on Progesterone Receptor (PGR) re-expression in the 4T1 TNBC cell line mouse model, using a comprehensive multiplex analysis. The study revealed a significant upregulation of PGR post-mEHT treatments, confirmed through immunostaining at the protein level. Additionally, we explored the therapeutic potential of Selective Progesterone Receptor Modulators (SPRMs), Mifepristone (MIF) and Ulipristal Acetate (UPA) to target re-expressed PGR *in vitro*. Our results suggested that mEHT-induced PGR re-activation may sensitize TNBC cells to SPRMs, offering a promising avenue for targeted therapy. Our findings indicate that mEHT not only restored endogenous functional PGR expression in TNBC cell line, but also re-sensitized TNBC cells to antiprogestins therapy.

8. References

1. Sung H, Ferlay J, Siegel RL, Laversanne M, Soerjomataram I, Jemal A, Bray F. Global Cancer Statistics 2020: GLOBOCAN Estimates of Incidence and Mortality Worldwide for 36 Cancers in 185 Countries. CA: A Cancer Journal for Clinicians. 2021;71(3):209-249.
2. Almansour NM. Triple-Negative Breast Cancer: A Brief Review About Epidemiology, Risk Factors, Signaling Pathways, Treatment and Role of Artificial Intelligence. Frontiers in Molecular Biosciences. 2022;9.
3. Foulkes WD, Smith IE, Reis-Filho JS. Triple-Negative Breast Cancer. New England Journal of Medicine. 2010;363(20):1938-1948.
4. Bianchini G, Balko JM, Mayer IA, Sanders ME, Gianni L. Triple-negative breast cancer: challenges and opportunities of a heterogeneous disease. Nat Rev Clin Oncol. 2016;13(11):674-690.
5. Yin L, Duan JJ, Bian XW, Yu SC. Triple-negative breast cancer molecular subtyping and treatment progress. Breast Cancer Res. 2020;22(1):61.
6. Smolarz B, Nowak AZ, Romanowicz H. Breast Cancer—Epidemiology, Classification, Pathogenesis and Treatment (Review of Literature). Cancers. 2022;14(10):2569.
7. Derakhshan F, Reis-Filho JS. Pathogenesis of Triple-Negative Breast Cancer. Annu Rev Pathol. 2022;17:181-204.
8. Dent R, Trudeau M, Pritchard KI, Hanna WM, Kahn HK, Sawka CA, Lickley LA, Rawlinson E, Sun P, Narod SA. Triple-Negative Breast Cancer: Clinical Features and Patterns of Recurrence. Clinical Cancer Research. 2007;13(15):4429-4434.
9. Lin NU, Claus E, Sohl J, Razzak AR, Arnaout A, Winer EP. Sites of distant recurrence and clinical outcomes in patients with metastatic triple-negative breast cancer: high incidence of central nervous system metastases. Cancer. 2008;113(10):2638-2645.
10. Le Du F, Ueno NT. Targeted Therapies in Triple-Negative Breast Cancer: Failure and Future. Women's Health. 2015;11(1):1-5.
11. Anders CK, Carey LA. Biology, metastatic patterns, and treatment of patients with triple-negative breast cancer. Clin Breast Cancer. 2009;9 Suppl 2(Suppl 2):S73-81.
12. MacDonald I, Nixon NA, Khan OF. Triple-Negative Breast Cancer: A Review of Current Curative Intent Therapies. Curr Oncol. 2022;29(7):4768-4778.

13. Le Breton L, Mayer MP. A model for handling cell stress. eLife. 2016;5:e22850.
14. Richter K, Haslbeck M, Buchner J. The Heat Shock Response: Life on the Verge of Death. Molecular Cell. 2010;40(2):253-266.
15. Morimoto RI. Cells in Stress: Transcriptional Activation of Heat Shock Genes. Science. 1993;259(5100):1409-1410.
16. Vihervaara A, Sistonen L. HSF1 at a glance. Journal of Cell Science. 2014;127(2):261-266.
17. Gumilar KE, Chin Y, Ibrahim IH, Tjokroprawiro BA, Yang J-Y, Zhou M, Gassman NR, Tan M. Heat Shock Factor 1 Inhibition: A Novel Anti-Cancer Strategy with Promise for Precision Oncology. Cancers. 2023;15(21):5167.
18. Ahmed K, Zaidi SF, Mati ur R, Rehman R, Kondo T. Hyperthermia and protein homeostasis: Cytoprotection and cell death. Journal of Thermal Biology. 2020;91:102615.
19. Wang X, Chen M, Zhou J, Zhang X. HSP27, 70 and 90, anti-apoptotic proteins, in clinical cancer therapy (Review). Int J Oncol. 2014;45(1):18-30.
20. Kijima T, Prince T, Neckers L, Koga F, Fujii Y. Heat shock factor 1 (HSF1)-targeted anticancer therapeutics: overview of current preclinical progress. Expert Opinion on Therapeutic Targets. 2019;23(5):369-377.
21. Hu C, Yang J, Qi Z, Wu H, Wang B, Zou F, Mei H, Liu J, Wang W, Liu Q. Heat shock proteins: Biological functions, pathological roles, and therapeutic opportunities. MedComm (2020). 2022;3(3):e161.
22. Parsell DA, Lindquist S. The function of heat-shock proteins in stress tolerance: degradation and reactivation of damaged proteins. Annu Rev Genet. 1993;27:437-496.
23. Rybiński M, Szymańska Z, Lasota S, Gambin A. Modelling the efficacy of hyperthermia treatment. Journal of The Royal Society Interface. 2013;10(88):20130527.
24. Jolly C, Morimoto RI. Role of the Heat Shock Response and Molecular Chaperones in Oncogenesis and Cell Death. JNCI: Journal of the National Cancer Institute. 2000;92(19):1564-1572.
25. Viana P, Hamar P. Targeting the heat shock response induced by modulated electro-hyperthermia (mEHT) in cancer. Biochimica et Biophysica Acta (BBA) - Reviews on Cancer. 2024;1879(2):189069.

26. Calderwood SK, Gong J. Heat Shock Proteins Promote Cancer: It's a Protection Racket. Trends Biochem Sci. 2016;41(4):311-323.
27. Tabuchi Y, Kondo T. Targeting heat shock transcription factor 1 for novel hyperthermia therapy (Review). Int J Mol Med. 2013;32(1):3-8.
28. Kohler V, Andréasson C. Reversible protein assemblies in the proteostasis network in health and disease. Frontiers in Molecular Biosciences. 2023;10.
29. Santagata S, Hu R, Lin NU, Mendillo ML, Collins LC, Hankinson SE, Schnitt SJ, Whitesell L, Tamimi RM, Lindquist S, Ince TA. High levels of nuclear heat-shock factor 1 (HSF1) are associated with poor prognosis in breast cancer. Proceedings of the National Academy of Sciences. 2011;108(45):18378-18383.
30. Whitesell L, Lindquist SL. HSP90 and the chaperoning of cancer. Nat Rev Cancer. 2005;5(10):761-772.
31. Dai C, Whitesell L, Rogers AB, Lindquist S. Heat Shock Factor 1 Is a Powerful Multifaceted Modifier of Carcinogenesis. Cell. 2007;130(6):1005-1018.
32. Calderwood SK, Khaleque MA, Sawyer DB, Ciocca DR. Heat shock proteins in cancer: chaperones of tumorigenesis. Trends in Biochemical Sciences. 2006;31(3):164-172.
33. Dai C, Sampson SB. HSF1: Guardian of Proteostasis in Cancer. Trends Cell Biol. 2016;26(1):17-28.
34. Powell CD, Paullin TR, Aoisa C, Menzie CJ, Ubaldini A, Westerheide SD. The Heat Shock Transcription Factor HSF1 Induces Ovarian Cancer Epithelial-Mesenchymal Transition in a 3D Spheroid Growth Model. PLOS ONE. 2016;11(12):e0168389.
35. Cyran AM, Zhitkovich A. Heat Shock Proteins and HSF1 in Cancer. Frontiers in Oncology. 2022;12.
36. Home T, Jensen RA, Rao R. Heat Shock Factor 1 in Protein Homeostasis and Oncogenic Signal Integration. Cancer Research. 2015;75(6):907-912.
37. Jiang S, Tu K, Fu Q, Schmitt DC, Zhou L, Lu N, Zhao Y. Multifaceted roles of HSF1 in cancer. Tumor Biology. 2015;36(7):4923-4931.
38. Chuma M, Sakamoto N, Nakai A, Hige S, Nakanishi M, Natsuizaka M, Suda G, Sho T, Hatanaka K, Matsuno Y, Yokoo H, Kamiyama T, Taketomi A, Fujii G, Tashiro K, Hikiba Y, Fujimoto M, Asaka M, Maeda S. Heat shock factor 1 accelerates

hepatocellular carcinoma development by activating nuclear factor-κB/mitogen-activated protein kinase. Carcinogenesis. 2013;35(2):272-281.

39. Fang F, Chang R, Yang L. Heat shock factor 1 promotes invasion and metastasis of hepatocellular carcinoma in vitro and in vivo. Cancer. 2012;118(7):1782-1794.

40. Engerud H, Tangen IL, Berg A, Kusonmano K, Halle MK, Øyan AM, Kalland KH, Stefansson I, Trovik J, Salvesen HB, Krakstad C. High level of HSF1 associates with aggressive endometrial carcinoma and suggests potential for HSP90 inhibitors. British Journal of Cancer. 2014;111(1):78-84.

41. Ishiwata J, Kasamatsu A, Sakuma K, Iyoda M, Yamatoji M, Usukura K, Ishige S, Shimizu T, Yamano Y, Ogawara K, Shiiba M, Tanzawa H, Uzawa K. State of heat shock factor 1 expression as a putative diagnostic marker for oral squamous cell carcinoma. Int J Oncol. 2012;40(1):47-52.

42. McConnell JR, Buckton LK, McAlpine SR. Regulating the master regulator: Controlling heat shock factor 1 as a chemotherapy approach. Bioorganic & Medicinal Chemistry Letters. 2015;25(17):3409-3414.

43. Carpenter RL, Gökmen-Polar Y. HSF1 as a Cancer Biomarker and Therapeutic Target. Curr Cancer Drug Targets. 2019;19(7):515-524.

44. Soo ETL, Yip GWC, Lwin ZM, Kumar SD, Bay B-H. Heat Shock Proteins as Novel Therapeutic Targets in Cancer. In Vivo. 2008;22(3):311-315.

45. Ciocca DR, Calderwood SK. Heat shock proteins in cancer: diagnostic, prognostic, predictive, and treatment implications. Cell Stress Chaperones. 2005;10(2):86-103.

46. Seclì L, Fusella F, Avalle L, Brancaccio M. The dark-side of the outside: how extracellular heat shock proteins promote cancer. Cellular and Molecular Life Sciences. 2021;78(9):4069-4083.

47. McConkey DJ. The integrated stress response and proteotoxicity in cancer therapy. Biochemical and Biophysical Research Communications. 2017;482(3):450-453.

48. Murphy ME. The HSP70 family and cancer. Carcinogenesis. 2013;34(6):1181-1188.

49. Elmallah MIY, Cordonnier M, Vautrot V, Chanteloup G, Garrido C, Gobbo J. Membrane-anchored heat-shock protein 70 (Hsp70) in cancer. Cancer Letters. 2020;469:134-141.

50. Joly A-L, Wettstein G, Mignot G, Ghiringhelli F, Garrido C. Dual Role of Heat Shock Proteins as Regulators of Apoptosis and Innate Immunity. Journal of Innate Immunity. 2010;2(3):238-247.

51. Albakova Z, Armeev GA, Kanevskiy LM, Kovalenko EI, Sapozhnikov AM. HSP70 Multi-Functionality in Cancer. Cells. 2020;9(3).

52. Yang S, Xiao H, Cao L. Recent advances in heat shock proteins in cancer diagnosis, prognosis, metabolism and treatment. Biomedicine & Pharmacotherapy. 2021;142:112074.

53. Vostakolaei MA, Abdolalizadeh J, Hejazi MS, Kordi S, Molavi O. Hsp70 in Cancer: Partner or Traitor to Immune System. Iran J Allergy Asthma Immunol. 2019;18(6):589-604.

54. Juhasz K, Lipp AM, Nimmervoll B, Sonnleitner A, Hesse J, Haselgruebler T, Balogi Z. The complex function of hsp70 in metastatic cancer. Cancers (Basel). 2013;6(1):42-66.

55. Du S, Liu Y, Yuan Y, Wang Y, Chen Y, Wang S, Chi Y. Advances in the study of HSP70 inhibitors to enhance the sensitivity of tumor cells to radiotherapy. Frontiers in Cell and Developmental Biology. 2022;10.

56. Cheng Y, Weng S, Yu L, Zhu N, Yang M, Yuan Y. The Role of Hyperthermia in the Multidisciplinary Treatment of Malignant Tumors. Integr Cancer Ther. 2019;18:1534735419876345.

57. Szasz A. Challenges and solutions in oncological hyperthermia. Thermal Medicine. 2013;29(1):1-23.

58. Harrison LE, Bryan M, Pliner L, Saunders T. Phase I Trial of Pegylated Liposomal Doxorubicin with Hyperthermic Intraperitoneal Chemotherapy in Patients Undergoing Cytoreduction for Advanced Intra-abdominal Malignancy. Annals of Surgical Oncology. 2008;15(5):1407-1413.

59. Dahl O. Interaction of hyperthermia and chemotherapy. Recent Results Cancer Res. 1988;107:157-169.

60. Los G, Smals OA, van Vugt MJ, van der Vlist M, den Engelse L, McVie JG, Pinedo HM. A rationale for carboplatin treatment and abdominal hyperthermia in cancers restricted to the peritoneal cavity. Cancer Res. 1992;52(5):1252-1258.

61. Jacquet P, Averbach A, Stuart OA, Chang D, Sugarbaker PH. Hyperthermic intraperitoneal doxorubicin: pharmacokinetics, metabolism, and tissue distribution in a rat model. Cancer Chemother Pharmacol. 1998;41(2):147-154.
62. Sugarbaker PH. Laboratory and clinical basis for hyperthermia as a component of intracavitary chemotherapy. International Journal of Hyperthermia. 2007;23(5):431-442.
63. Lee SY, Fiorentini G, Szasz AM, Szigeti G, Szasz A, Minnaar CA. Quo Vadis Oncological Hyperthermia (2020)? Front Oncol. 2020;10:1690.
64. Szasz A, Szasz N, Szasz O. Oncothermia: principles and practices: Springer Science & Business Media; 2010.
65. Lee S-Y, Szigeti GP, Szasz AM. Oncological hyperthermia: The correct dosing in clinical applications. Int J Oncol. 2019;54(2):627-643.
66. Hegyi G, Szigeti GP, Szász A. Hyperthermia versus Oncothermia: Cellular Effects in Complementary Cancer Therapy. Evidence-Based Complementary and Alternative Medicine. 2013;2013:672873.
67. Mosser DD, Morimoto RI. Molecular chaperones and the stress of oncogenesis. Oncogene. 2004;23(16):2907-2918.
68. Calderwood SK, Asea A. Targeting HSP70 induced thermotolerance for design of thermal sensitizers. International Journal of Hyperthermia. 2002;18(6):597-608.
69. Chen K, Qian W, Li J, Jiang Z, Cheng L, Yan B, Cao J, Sun L, Zhou C, Lei M, Duan W, Ma J, Ma Q, Ma Z. Loss of AMPK activation promotes the invasion and metastasis of pancreatic cancer through an HSF1-dependent pathway. Mol Oncol. 2017;11(10):1475-1492.
70. Liang W, Liao Y, Zhang J, Huang Q, Luo W, Yu J, Gong J, Zhou Y, Li X, Tang B, He S, Yang J. Heat shock factor 1 inhibits the mitochondrial apoptosis pathway by regulating second mitochondria-derived activator of caspase to promote pancreatic tumorigenesis. J Exp Clin Cancer Res. 2017;36(1):64.
71. Heimberger T, Andrulis M, Riedel S, Stühmer T, Schraud H, Beilhack A, Bumm T, Bogen B, Einsele H, Bargou RC, Chatterjee M. The heat shock transcription factor 1 as a potential new therapeutic target in multiple myeloma. British Journal of Haematology. 2013;160(4):465-476.
72. Li J, Song P, Jiang T, Dai D, Wang H, Sun J, Zhu L, Xu W, Feng L, Shin VY, Morrison H, Wang X, Jin H. Heat Shock Factor 1 Epigenetically Stimulates Glutaminase-

1-Dependent mTOR Activation to Promote Colorectal Carcinogenesis. Mol Ther. 2018;26(7):1828-1839.

73. Nakamura Y, Fujimoto M, Fukushima S, Nakamura A, Hayashida N, Takii R, Takaki E, Nakai A, Muto M. Heat shock factor 1 is required for migration and invasion of human melanoma in vitro and in vivo. Cancer Letters. 2014;354(2):329-335.

74. Mendillo Marc L, Santagata S, Koeva M, Bell George W, Hu R, Tamimi Rulla M, Fraenkel E, Ince TA, Whitesell L, Lindquist S. HSF1 Drives a Transcriptional Program Distinct from Heat Shock to Support Highly Malignant Human Cancers. Cell. 2012;150(3):549-562.

75. Xi C, Hu Y, Buckhaults P, Moskophidis D, Mivechi NF. Heat shock factor Hsf1 cooperates with ErbB2 (Her2/Neu) protein to promote mammary tumorigenesis and metastasis. J Biol Chem. 2012;287(42):35646-35657.

76. Dai C, Santagata S, Tang Z, Shi J, Cao J, Kwon H, Bronson RT, Whitesell L, Lindquist S. Loss of tumor suppressor NF1 activates HSF1 to promote carcinogenesis. J Clin Invest. 2012;122(10):3742-3754.

77. Gabai VL, Meng L, Kim G, Mills TA, Benjamin IJ, Sherman MY. Heat shock transcription factor Hsf1 is involved in tumor progression via regulation of hypoxia-inducible factor 1 and RNA-binding protein HuR. Mol Cell Biol. 2012;32(5):929-940.

78. Cigliano A, Wang C, Pilo MG, Szydlowska M, Brozzetti S, Latte G, Pes GM, Pascale RM, Seddaiu MA, Vidili G, Ribback S, Dombrowski F, Evert M, Chen X, Calvisi DF. Inhibition of HSF1 suppresses the growth of hepatocarcinoma cell lines in vitro and AKT-driven hepatocarcinogenesis in mice. Oncotarget. 2017;8(33):54149-54159.

79. Li S, Ma W, Fei T, Lou Q, Zhang Y, Cui X, Qin X, Zhang J, Liu G, Dong Z, Ma Y, Song Z, Hu Y. Upregulation of heat shock factor 1 transcription activity is associated with hepatocellular carcinoma progression. Mol Med Rep. 2014;10(5):2313-2321.

80. Rossi A, Ciafrè S, Balsamo M, Pierimarchi P, Santoro MG. Targeting the Heat Shock Factor 1 by RNA Interference: A Potent Tool to Enhance Hyperthermochemotherapy Efficacy in Cervical Cancer. Cancer Research. 2006;66(15):7678-7685.

81. Nakamura Y, Fujimoto M, Hayashida N, Takii R, Nakai A, Muto M. Silencing HSF1 by short hairpin RNA decreases cell proliferation and enhances sensitivity to

hyperthermia in human melanoma cell lines. Journal of Dermatological Science. 2010;60(3):187-192.

82. Wang X, Zhang D, Cao M, Ba J, Wu B, Liu T, Nie C. A study on the biological function of heat shock factor 1 proteins in breast cancer. Oncol Lett. 2018;16(3):3145-3149.

83. Meng L, Gabai VL, Sherman MY. Heat-shock transcription factor HSF1 has a critical role in human epidermal growth factor receptor-2-induced cellular transformation and tumorigenesis. Oncogene. 2010;29(37):5204-5213.

84. Desai S, Liu Z, Yao J, Patel N, Chen J, Wu Y, Ahn EEY, Fodstad O, Tan M. Heat shock factor 1 (HSF1) controls chemoresistance and autophagy through transcriptional regulation of autophagy-related protein 7 (ATG7). J Biol Chem. 2013;288(13):9165-9176.

85. Wang JH, Yao MZ, Gu JF, Sun LY, Shen YF, Liu XY. Blocking HSF1 by dominant-negative mutant to sensitize tumor cells to hyperthermia. Biochem Biophys Res Commun. 2002;290(5):1454-1461.

86. Tabuchi Y, Furusawa Y, Wada S, Ohtsuka K, Kondo T. Silencing Heat Shock Transcription Factor 1 Using Small Interfering RNA Enhances Mild Hyperthermia and Hyperthermia Sensitivity in Human Oral Squamous Cell Carcinoma Cells. Thermal Medicine. 2011;27(4):99-108.

87. Zhang Y, Huang L, Zhang J, Moskophidis D, Mivechi NF. Targeted disruption of hsf1 leads to lack of thermotolerance and defines tissue-specific regulation for stress-inducible Hsp molecular chaperones. J Cell Biochem. 2002;86(2):376-393.

88. McMillan DR, Xiao X, Shao L, Graves K, Benjamin IJ. Targeted Disruption of Heat Shock Transcription Factor 1 Abolishes Thermotolerance and Protection against Heat-inducible Apoptosis*. Journal of Biological Chemistry. 1998;273(13):7523-7528.

89. Schvarcz CA, Danics L, Krenács T, Viana P, Béres R, Vancsik T, Nagy A, Gyenesei A, Kun J, Fonović M, Vidmar R, Benyó Z, Kaucsár T, Hamar Péter. Modulated Electro-Hyperthermia Induces a Prominent Local Stress Response and Growth Inhibition in Mouse Breast Cancer Isografts. Cancers (Basel). 2021;13(7).

90. Danics L, Schvarcz CA, Viana P, Vancsik T, Krenács T, Benyó Z, Kaucsár T, Hamar Péter. Exhaustion of Protective Heat Shock Response Induces Significant Tumor

Damage by Apoptosis after Modulated Electro-Hyperthermia Treatment of Triple Negative Breast Cancer Isografts in Mice. Cancers (Basel). 2020;12(9).

91. Fiorentini G, Sarti D, Milandri C, Dentico P, Mambrini A, Fiorentini C, Mattioli G, Casadei V, Guadagni S. Modulated Electrohyperthermia in Integrative Cancer Treatment for Relapsed Malignant Glioblastoma and Astrocytoma: Retrospective Multicenter Controlled Study. Integr Cancer Ther. 2019;18:1534735418812691.

92. Minnaar CA, Kotzen JA, Ayeni OA, Naidoo T, Tunmer M, Sharma V, Vangu MDT, Baeyens A. The effect of modulated electro-hyperthermia on local disease control in HIV-positive and -negative cervical cancer women in South Africa: Early results from a phase III randomised controlled trial. PLoS One. 2019;14(6):e0217894.

93. Zimmerman JW, Jimenez H, Pennison MJ, Brezovich I, Morgan D, Mudry A, Costa FP, Barbault A, Pasche B. Targeted treatment of cancer with radiofrequency electromagnetic fields amplitude-modulated at tumor-specific frequencies. Chin J Cancer. 2013;32(11):573-581.

94. Papp E, Vancsik T, Kiss E, Szasz O. Energy Absorption by the Membrane Rafts in the Modulated Electro-Hyperthermia (mEHT). Open Journal of Biophysics. 2017;07(04):216-229.

95. Andocs G, Rehman MU, Zhao QL, Tabuchi Y, Kanamori M, Kondo T. Comparison of biological effects of modulated electro-hyperthermia and conventional heat treatment in human lymphoma U937 cells. Cell Death Discov. 2016;2:16039.

96. Alshaibi HF, Al-shehri B, Hassan B, Al-zahrani R, Assiss T. Modulated Electrohyperthermia: A New Hope for Cancer Patients. BioMed Research International. 2020;2020:8814878.

97. Attila Marcell Szász GL, András Szász, Gyula Szigeti. The Immunogenic Connection of Thermal and Nonthermal Molecular Effects in Modulated Electro-Hyperthermia. Open Journal of Biophysics. 2023;13:103-142.

98. Szasz A. Thermal and nonthermal effects of radiofrequency on living state and applications as an adjuvant with radiation therapy. Journal of Radiation and Cancer Research. 2019;10(1):1-17.

99. Szasz O, Andocs G, Meggyeshazi N. Modulation Effect in Oncothermia. Conference Papers in Medicine. 2013;2013:398678.

100. Szasz A, Szasz N, Szasz O. Oncothermia – A New Kind of Oncologic Hyperthermia. In: Szasz A, Szasz N, Szasz O, editors. Oncothermia: Principles and Practices. Dordrecht: Springer Netherlands; 2011. p. 173-392.

101. Andocs G, Szasz O, Szasz A. Oncothermia treatment of cancer: from the laboratory to clinic. Electromagn Biol Med. 2009;28(2):148-165.

102. Szasz O, Szasz MA, Minnaar C, Szasz A. Heating Preciosity - Trends in Modern Oncological Hyperthermia. Open Journal of Biophysics. 2017;Vol.07No.03:29.

103. Andocs G, Renner H, Balogh L, Fonyad L, Jakab C, Szasz A. Strong synergy of heat and modulated electromagnetic field in tumor cell killing. Strahlenther Onkol. 2009;185(2):120-126.

104. Roussakow S. The History of Hyperthermia Rise and Decline. Conference Papers in Medicine. 2013;2013:428027.

105. Yang K-L, Huang C-C, Chi M-S, Chiang H-C, Wang Y-S, Hsia C-C, Andocs G, Wang HE, Chi KH. In vitro comparison of conventional hyperthermia and modulated electro-hyperthermia. Oncotarget. 2016;7(51).

106. Vancsik T, Kovago C, Kiss E, Papp E, Forika G, Benyo Z, Meggyeshazi N, Krenacs T. Modulated electro-hyperthermia induced loco-regional and systemic tumor destruction in colorectal cancer allografts. J Cancer. 2018;9(1):41-53.

107. Tsang YW, Chi KH, Huang CC, Chi MS, Chiang HC, Yang KL, Li WT, Wang YS. Modulated electro-hyperthermia-enhanced liposomal drug uptake by cancer cells. Int J Nanomedicine. 2019;14:1269-1279.

108. Nagata T, Kanamori M, Sekine S, Arai M, Moriyama M, Fujii T. Clinical study of modulated electro-hyperthermia for advanced metastatic breast cancer. Mol Clin Oncol. 2021;14(5):103.

109. Minnaar CA, Maposa I, Kotzen JA, Baeyens A. Effects of Modulated Electro-Hyperthermia (mEHT) on Two and Three Year Survival of Locally Advanced Cervical Cancer Patients. Cancers (Basel). 2022;14(3).

110. Yoo HJ, Lim MC, Seo S-S, Kang S, Joo J, Park S-Y. Phase I/II clinical trial of modulated electro-hyperthermia treatment in patients with relapsed, refractory or progressive heavily treated ovarian cancer. Japanese Journal of Clinical Oncology. 2019;49(9):832-838.

111. Kim S, Lee JH, Cha J, You SH. Beneficial effects of modulated electro-hyperthermia during neoadjuvant treatment for locally advanced rectal cancer. International Journal of Hyperthermia. 2021;38(1):144-151.

112. Fiorentini G, Sarti D, Casadei V, Milandri C, Dentico P, Mambrini A, Nani R, Fiorentini C, Guadagni S. Modulated Electro-Hyperthermia as Palliative Treatment for Pancreatic Cancer: A Retrospective Observational Study on 106 Patients. Integr Cancer Ther. 2019;18:1534735419878505.

113. Fiorentini G, Sarti D, Ranieri G, Gadaleta CD, Fiorentini C, Milandri C, Mambrini A, Guadagni S. Modulated electro-hyperthermia in stage III and IV pancreatic cancer: Results of an observational study on 158 patients. World J Clin Oncol. 2021;12(11):1064-1071.

114. Petenyi FG, Garay T, Muhl D, Izso B, Karaszi A, Borbenyi E, Herold M, Herold Z, Szasz AM, Dank M. Modulated Electro-Hyperthermic (mEHT) Treatment in the Therapy of Inoperable Pancreatic Cancer Patients-A Single-Center Case-Control Study. Diseases. 2021;9(4).

115. Luo Z, Zheng K, Fan Q, Jiang X, Xiong D. Hyperthermia exposure induces apoptosis and inhibits proliferation in HCT116 cells by upregulating miR-34a and causing transcriptional activation of p53. Exp Ther Med. 2017;14(6):5379-5386.

116. Szasz A. Heterogeneous Heat Absorption Is Complementary to Radiotherapy. Cancers. 2022;14(4):901.

117. Vancsik T, Forika G, Balogh A, Kiss E, Krenacs T. Modulated electro-hyperthermia induced p53 driven apoptosis and cell cycle arrest additively support doxorubicin chemotherapy of colorectal cancer in vitro. Cancer Med. 2019;8(9):4292-4303.

118. Lee S-Y, Kim J-H, Han Y-H, Cho D-H. The effect of modulated electro-hyperthermia on temperature and blood flow in human cervical carcinoma. International Journal of Hyperthermia. 2018;34(7):953-960.

119. Lepock JR. Role of nuclear protein denaturation and aggregation in thermal radiosensitization. International Journal of Hyperthermia. 2004;20(2):115-130.

120. Krenacs T, Meggyeshazi N, Forika G, Kiss E, Hamar P, Szekely T, Vancsik T. Modulated Electro-Hyperthermia-Induced Tumor Damage Mechanisms Revealed in Cancer Models. Int J Mol Sci. 2020;21(17).

121. Elming PB, Sørensen BS, Oei AL, Franken NAP, Crezee J, Overgaard J, Horsman MR. Hyperthermia: The Optimal Treatment to Overcome Radiation Resistant Hypoxia. Cancers (Basel). 2019;11(1).
122. Vaupel P, Piazena H, Notter M, Thomsen AR, Grosu AL, Scholkmann F, Pockley AG, Multhoff G. From Localized Mild Hyperthermia to Improved Tumor Oxygenation: Physiological Mechanisms Critically Involved in Oncologic Thermo-Radio-Immunotherapy. Cancers (Basel). 2023;15(5).
123. Minnaar CA, Kotzen JA, Naidoo T, Tunmer M, Sharma V, Vangu M-D-T, Baeyens A. Analysis of the effects of mEHT on the treatment-related toxicity and quality of life of HIV-positive cervical cancer patients. International Journal of Hyperthermia. 2020;37(1):263-272.
124. Foster KR. Thermal and nonthermal mechanisms of interaction of radio-frequency energy with biological systems. IEEE Transactions on Plasma Science. 2000;28(1):15-23.
125. Szasz A, Szasz O, Szasz N. Electro-hyperthermia: a New Paradigm in Cancer Therapy. Deutsche Zeitschrift für Onkologie. 2001;33(03):91-99.
126. Deipolyi AR, Golberg A, Yarmush ML, Arellano RS, Oklu R. Irreversible electroporation: evolution of a laboratory technique in interventional oncology. Diagn Interv Radiol. 2014;20(2):147-154.
127. Sasaki K, Porter E, Rashed EA, Farrugia L, Schmid G. Measurement and image-based estimation of dielectric properties of biological tissues -past, present, and future. Phys Med Biol. 2022;67(14).
128. Szasz A. Time-Fractal Modulation—Possible Modulation Effects in Human Therapy. Open Journal of Biophysics. 2022;12:38-87.
129. Mousavi M, Baharara J, Shahrokhabadi K. The Synergic Effects of Crocus Sativus L. and Low Frequency Electromagnetic Field on VEGFR2 Gene Expression in Human Breast Cancer Cells. Avicenna J Med Biotechnol. 2014;6(2):123-127.
130. Qin W, Akutsu Y, Andocs G, Suganami A, Hu X, Yusup G, Komatsu-Akimoto A, Hoshino I, Hanari N, Mori M, Isozaki Y, Akanuma N, Tamura Y, Matsubara H. Modulated electro-hyperthermia enhances dendritic cell therapy through an abscopal effect in mice. Oncol Rep. 2014;32(6):2373-2379.

131. Minnaar CA, Szasz A. Forcing the Antitumor Effects of HSPs Using a Modulated Electric Field. Cells. 2022;11(11):1838.
132. Tsang YW, Huang CC, Yang KL, Chi MS, Chiang HC, Wang YS, Andocs G, Szasz A, Li WT, Chi KH. Improving immunological tumor microenvironment using electro-hyperthermia followed by dendritic cell immunotherapy. BMC Cancer. 2015;15:708.
133. Vancsik T, Máthé D, Horváth I, Várallyaly AA, Benedek A, Bergmann R, Andocs G, Szasz A, Li WT, Chi KH. Modulated Electro-Hyperthermia Facilitates NK-Cell Infiltration and Growth Arrest of Human A2058 Melanoma in a Xenograft Model. Frontiers in Oncology. 2021;11.
134. Lee S-Y, Lorant G, Grand L, Szasz AM. The Clinical Validation of Modulated Electro-Hyperthermia (mEHT). Cancers. 2023;15(18):4569.
135. Chi MS, Mehta MP, Yang KL, Lai HC, Lin YC, Ko HL, Wang YS, Liao KW, Chi KH. Putative Abscopal Effect in Three Patients Treated by Combined Radiotherapy and Modulated Electrohyperthermia. Front Oncol. 2020;10:254.
136. Chi M-S, Wu J-H, Shaw S, Wu C-J, Chen L-K, Hsu H-C, Chi KH. Marked local and distant response of heavily treated breast cancer with cardiac metastases treated by combined low dose radiotherapy, low dose immunotherapy and hyperthermia: a case report. Therapeutic Radiology and Oncology. 2021;5.
137. Andocs G, Meggyeshazi N, Balogh L, Spisak S, Maros ME, Balla P, Kiszner G, Teleki I, Kovago C, Krenacs T. Upregulation of heat shock proteins and the promotion of damage-associated molecular pattern signals in a colorectal cancer model by modulated electrohyperthermia. Cell Stress Chaperones. 2015;20(1):37-46.
138. Meggyesházi N, Andócs G, Spisák S, Krenács T. Early Changes in mRNA and Protein Expression Related to Cancer Treatment by Modulated Electrohyperthermia. Conference Papers in Medicine. 2013;2013:249563.
139. Besztercei B, Vancsik T, Benedek A, Major E, Thomas MJ, Schvarcz CA, Krenács T, Benyó Z, Balogh A. Stress-Induced, p53-Mediated Tumor Growth Inhibition of Melanoma by Modulated Electrohyperthermia in Mouse Models without Major Immunogenic Effects. Int J Mol Sci. 2019;20(16).
140. Kuo IM, Lee JJ, Wang YS, Chiang HC, Huang CC, Hsieh PJ, Han W, Ke CH, Liao ATC, Lin CS. Potential enhancement of host immunity and anti-tumor efficacy of

nanoscale curcumin and resveratrol in colorectal cancers by modulated electro-hyperthermia. BMC Cancer. 2020;20(1):603.

141. Forika G, Kiss E, Petovari G, Danko T, Gellert AB, Krenacs T. Modulated Electro-Hyperthermia Supports the Effect of Gemcitabine Both in Sensitive and Resistant Pancreas Adenocarcinoma Cell Lines. Pathol Oncol Res. 2021;27:1610048.

142. Dutta N, Pal K, Pal M. Heat Shock Factor 1 and Its Small Molecule Modulators with Therapeutic Potential. In: Asea AAA, Kaur P, editors. Heat Shock Proteins in Inflammatory Diseases. Cham: Springer International Publishing; 2021. p. 69-88.

143. Chin Y, Gumilar KE, Li XG, Tjokroprawiro BA, Lu CH, Lu J, Zhou M, Sobol RW, Tan M. Targeting HSF1 for cancer treatment: mechanisms and inhibitor development. Theranostics. 2023;13(7):2281-2300.

144. Kim SJ, Lee SC, Kang HG, Gim J, Lee KH, Lee SH, Chun KH. Heat Shock Factor 1 Predicts Poor Prognosis of Gastric Cancer. Yonsei Med J. 2018;59(9):1041-1048.

145. Chatterjee S, Burns TF. Targeting Heat Shock Proteins in Cancer: A Promising Therapeutic Approach. Int J Mol Sci. 2017;18(9).

146. Dong B, Jaeger AM, Thiele DJ. Inhibiting Heat Shock Factor 1 in Cancer: A Unique Therapeutic Opportunity. Trends in Pharmacological Sciences. 2019;40(12):986-1005.

147. Sharma C, Seo YH. Small Molecule Inhibitors of HSF1-Activated Pathways as Potential Next-Generation Anticancer Therapeutics. Molecules. 2018;23(11).

148. Yoon YJ, Kim JA, Shin KD, Shin DS, Han YM, Lee YJ, Lee JS, Kwon BM, Han DC. KRIBB11 inhibits HSP70 synthesis through inhibition of heat shock factor 1 function by impairing the recruitment of positive transcription elongation factor b to the hsp70 promoter. J Biol Chem. 2011;286(3):1737-1747.

149. Yallowitz A, Ghaleb A, Garcia L, Alexandrova EM, Marchenko N. Heat shock factor 1 confers resistance to lapatinib in ERBB2-positive breast cancer cells. Cell Death & Disease. 2018;9(6):621.

150. Carpenter RL, Sirkisoon S, Zhu D, Rimkus T, Harrison A, Anderson A, Paw I, Qasem S, Xing F, Liu Y, Chan M, Metheny-Barlow L, Pasche BC, Debinski W, Watabe K, Lo HW. Combined inhibition of AKT and HSF1 suppresses breast cancer stem cells and tumor growth. Oncotarget. 2017;8(43):73947-73963.

151. Yang T, Ren C, Lu C, Qiao P, Han X, Wang L, Wang D, Lv S, Sun Y, Yu Z. Phosphorylation of HSF1 by PIM2 Induces PD-L1 Expression and Promotes Tumor Growth in Breast Cancer. Cancer Res. 2019;79(20):5233-5244.
152. Tandon V, Moreno R, Allmeroth K, Quinn J, Wiley SE, Nicely LG, Denzel MS, Edwards J, de la Vega L, Banerjee S. Dual inhibition of HSF1 and DYRK2 impedes cancer progression. Biosci Rep. 2023;43(1).
153. Huang M, Dong W, Xie R, Wu J, Su Q, Li W, Yao K, Chen Y, Zhou Q, Zhang Q, Li W, Cheng L, Peng S, Chen S, Huang J, Chen X, Lin T. HSF1 facilitates the multistep process of lymphatic metastasis in bladder cancer via a novel PRMT5-WDR5-dependent transcriptional program. Cancer Commun (Lond). 2022;42(5):447-470.
154. Lee S, Jung J, Lee YJ, Kim SK, Kim JA, Kim BK, Park KC, Kwon BM, Han DC. Targeting HSF1 as a Therapeutic Strategy for Multiple Mechanisms of EGFR Inhibitor Resistance in EGFR Mutant Non-Small-Cell Lung Cancer. Cancers (Basel). 2021;13(12).
155. Shen Z, Yin L, Zhou H, Ji X, Jiang C, Zhu X, He X. Combined inhibition of AURKA and HSF1 suppresses proliferation and promotes apoptosis in hepatocellular carcinoma by activating endoplasmic reticulum stress. Cellular Oncology. 2021;44(5):1035-1049.
156. Fok JHL, Hedayat S, Zhang L, Aronson LI, Mirabella F, Pawlyn C, Bright MD, Wardell CP, Keats JJ, De Billy E, Rye CS, Chessum NEA, Jones K, Morgan GJ, Eccles SA, Workman P, Davies FE. HSF1 Is Essential for Myeloma Cell Survival and A Promising Therapeutic Target. Clin Cancer Res. 2018;24(10):2395-2407.
157. Antonietti P, Linder B, Hehlgans S, Mildenberger IC, Burger MC, Fulda S, Steinbach JP, Gessler F, Rödel F, Mittelbronn M, Kögel D. Interference with the HSF1/HSP70/BAG3 Pathway Primes Glioma Cells to Matrix Detachment and BH3 Mimetic–Induced Apoptosis. Molecular Cancer Therapeutics. 2017;16(1):156-168.
158. Ishikawa C, Mori N. Heat shock factor 1 is a promising therapeutic target against adult T-cell leukemia. Medical Oncology. 2023;40(6):172.
159. Yoo K, Yun HH, Jung SY, Lee JH. KRIBB11 Induces Apoptosis in A172 Glioblastoma Cells via MULE-Dependent Degradation of MCL-1. Molecules. 2021;26(14).
160. Grimm SL, Hartig SM, Edwards DP. Progesterone Receptor Signaling Mechanisms. Journal of Molecular Biology. 2016;428(19):3831-3849.

161. Islam MS, Afrin S, Jones SI, Segars J. Selective Progesterone Receptor Modulators-Mechanisms and Therapeutic Utility. Endocr Rev. 2020;41(5).

162. Cenciarini ME, Proietti CJ. Molecular mechanisms underlying progesterone receptor action in breast cancer: Insights into cell proliferation and stem cell regulation. Steroids. 2019;152:108503.

163. Li Z, Wei H, Li S, Wu P, Mao X. The Role of Progesterone Receptors in Breast Cancer. Drug Des Devel Ther. 2022;16:305-314.

164. Graham JD, Yager ML, Hill HD, Byth K, O'Neill GM, Clarke CL. Altered Progesterone Receptor Isoform Expression Remodels Progestin Responsiveness of Breast Cancer Cells. Molecular Endocrinology. 2005;19(11):2713-2735.

165. Sohail SK, Sarfraz R, Imran M, Kamran M, Qamar S. Estrogen and Progesterone Receptor Expression in Breast Carcinoma and Its Association With Clinicopathological Variables Among the Pakistani Population. Cureus. 2020;12(8):e9751.

166. Azeez JM, Susmi TR, Remadevi V, Ravindran V, Sasikumar Sujatha A, Ayswarya RNS, Sreeja S. New insights into the functions of progesterone receptor (PR) isoforms and progesterone signaling. Am J Cancer Res. 2021;11(11):5214-5232.

167. Poole AJ, Li Y, Kim Y, Lin S-CJ, Lee W-H, Lee EY-HP. Prevention of Brca-Mediated Mammary Tumorigenesis in Mice by a Progesterone Antagonist. Science. 2006;314(5804):1467-1470.

168. Lee O, Sullivan ME, Xu Y, Rogers C, Muzzio M, Helenowski I, Shidfar A, Zeng Z, Singhal H, Jovanovic B, Hansen N, Bethke KP, Gann PH, Gradishar W, Kim JJ, Clare SE, Khan SA. Selective Progesterone Receptor Modulators in Early-Stage Breast Cancer: A Randomized, Placebo-Controlled Phase II Window-of-Opportunity Trial Using Telapristone Acetate. Clinical Cancer Research. 2020;26(1):25-34.

169. Lange CA, Yee D. Progesterone and breast cancer. Womens Health (Lond). 2008;4(2):151-162.

170. Bardou VJ, Arpino G, Elledge RM, Osborne CK, Clark GM. Progesterone receptor status significantly improves outcome prediction over estrogen receptor status alone for adjuvant endocrine therapy in two large breast cancer databases. J Clin Oncol. 2003;21(10):1973-1979.

171. Xiao Y, Li J, Wu Z, Zhang X, Ming J. Influence of progesterone receptor on metastasis and prognosis in breast cancer patients with negative HER-2. Gland Surgery. 2022;11(1):77-90.
172. Fan Y, Ding X, Xu B, Ma F, Yuan P, Wang J, Zhang P, Li Q, Luo Y. Prognostic Significance of Single Progesterone Receptor Positivity: A Comparison Study of Estrogen Receptor Negative/Progesterone Receptor Positive/Her2 Negative Primary Breast Cancer With Triple Negative Breast Cancer. Medicine. 2015;94(46):e2066.
173. Davey MG, Ryan É J, Folan PJ, O'Halloran N, Boland MR, Barry MK, Sweeney KJ, Malone CM, McLaughlin RJ, Kerin MJ, Lowery AJ. The impact of progesterone receptor negativity on oncological outcomes in oestrogen-receptor-positive breast cancer. BJS Open. 2021;5(3).
174. Boland MR, Ryan ÉJ, Dunne E, Aherne TM, Bhatt NR, Lowery AJ. Meta-analysis of the impact of progesterone receptor status on oncological outcomes in oestrogen receptor-positive breast cancer. British Journal of Surgery. 2019;107(1):33-43.
175. Riss TL, Moravec RA, Niles AL, Duellman S, Benink HA, Worzella TJ, Minor L. Cell Viability Assays. In: Markossian S, Grossman A, Brimacombe K, Arkin M, Auld D, Austin C, Baell J, Brimacombe K, Chung TDY, Coussens NP, Dahlin JL, Devanarayan V, Foley TL, Glicksman M, Gorshkov K, Haas JV, Hall MD, Hoare S, Inglese J, Iversen PW, Lal-Nag M, Li Z, Manro JR, McGee J, McManus O, Pearson M, Riss T, Saradjian P, Sittampalam GS, Tarselli M, Trask OJ, Weidner JR, Wildey MJ, Wilson K, Xia M, Xu X, editors. Assay Guidance Manual. Bethesda (MD): Eli Lilly & Company and the National Center for Advancing Translational Sciences; 2004.
176. Viana PHL, Schvarcz CA, Danics LO, Besztercei B, Aloss K, Bokhari SMZ, Giunashvili N, Bócsi D, Koós Z, Benyó Z, Hamar P. Heat shock factor 1 inhibition enhances the effects of modulated electro hyperthermia in a triple negative breast cancer mouse model. Scientific Reports. 2024;14(1):8241.
177. Zhang GL, Zhang Y, Cao KX, Wang XM. Orthotopic Injection of Breast Cancer Cells into the Mice Mammary Fat Pad. J Vis Exp. 2019(143).
178. Jin X, Moskophidis D, Mivechi NF. Heat shock transcription factor 1 is a key determinant of HCC development by regulating hepatic steatosis and metabolic syndrome. Cell Metab. 2011;14(1):91-103.

179. Lu X, Guo Y, Gu S, Tan D, Cheng B, Li Z, Huang W. An efficient and precise method for generating knockout cell lines based on CRISPR-Cas9 system. Engineering in Life Sciences. 2020;20(12):585-593.

180. Han X, Liu Z, Jo Mc, Zhang K, Li Y, Zeng Z, Li N, Zu Y, Qin L. CRISPR-Cas9 delivery to hard-to-transfect cells via membrane deformation. Science Advances. 2015;1(7):e1500454.

181. Gabai VL, Meng L, Kim G, Mills TA, Benjamin IJ, Sherman MY. Heat Shock Transcription Factor Hsf1 Is Involved in Tumor Progression via Regulation of Hypoxia-Inducible Factor 1 and RNA-Binding Protein HuR. Molecular and Cellular Biology. 2012;32(5):929-940.

182. Zorzi E, Bonvini P. Inducible Hsp70 in the Regulation of Cancer Cell Survival: Analysis of Chaperone Induction, Expression and Activity. Cancers. 2011;3(4):3921-3956.

183. Wigmore SJ, Sangster K, McNally SJ, Harrison EM, Ross JA, Fearon KCH, Garden OJ. De-repression of heat shock transcription factor-1 in interleukin-6- treated hepatocytes is mediated by downregulation of glycogen synthase kinase 3β and MAPK/ERK-1. Int J Mol Med. 2007;19(3):413-420.

184. Shen Z, Yin L, Zhou H, Ji X, Jiang C, Zhu X, He X. Combined inhibition of AURKA and HSF1 suppresses proliferation and promotes apoptosis in hepatocellular carcinoma by activating endoplasmic reticulum stress. Cell Oncol (Dordr). 2021;44(5):1035-1049.

185. Li J, Labbadia J, Morimoto RI. Rethinking HSF1 in Stress, Development, and Organismal Health. Trends Cell Biol. 2017;27(12):895-905.

186. Simões RV, Serganova IS, Kruchevsky N, Leftin A, Shestov AA, Thaler HT, Sukenick G, Locasale JW, Blasberg RG, Koutcher JA, Ackerstaff E. Metabolic plasticity of metastatic breast cancer cells: adaptation to changes in the microenvironment. Neoplasia. 2015;17(8):671-684.

187. Lee SY, Ju MK, Jeon HM, Jeong EK, Lee YJ, Kim CH, Park HG, Han SI, Kang HS. Regulation of Tumor Progression by Programmed Necrosis. Oxid Med Cell Longev. 2018;2018:3537471.

188. Schrörs B, Boegel S, Albrecht C, Bukur T, Bukur V, Holtsträter C, Ritzel C, Manninen K, Tadmor AD, Vormehr M, Sahin U, Löwer M. Multi-Omics

Characterization of the 4T1 Murine Mammary Gland Tumor Model. Frontiers in Oncology. 2020;10.

189. Tieszen CR, Goyeneche AA, Brandhagen BN, Ortbahn CT, Telleria CM. Antiprogestin mifepristone inhibits the growth of cancer cells of reproductive and non-reproductive origin regardless of progesterone receptor expression. BMC Cancer. 2011;11:207.

190. Wargon V, Fernandez SV, Goin M, Giulianelli S, Russo J, Lanari C. Hypermethylation of the progesterone receptor A in constitutive antiprogestin-resistant mouse mammary carcinomas. Breast Cancer Res Treat. 2011;126(2):319-332.

9. Publications

The dissertation is based on the following publications

Viana, P.H.L., Schvarcz, C.A., Danics, L.O., Besztercei, B., Aloss, K., Bokhari, S.M.Z., Giunashvili, N., Bócsi, D., Koós, Z., Benyó, Z., Hamar, P. Reviving Hormonal Signaling: mEHT-Driven Progesterone Receptor Re-Expression in Triple-Negative Breast Cancer Mouse Model and Antiprogestin Potentiation for Targeted Breast Cancer Treatment. **To be submitted**.

Viana, P.H.L., Schvarcz, C.A., Danics, L.O., Besztercei, B., Aloss, K., Bokhari, S.M.Z., Giunashvili, N., Bócsi, D., Koós, Z., Benyó, Z., Hamar, P. (2024) Heat shock factor 1 inhibition enhances the effects of modulated electro hyperthermia in a triple negative breast cancer mouse model. Sci Rep 14:8241. Doi: 10.1038/s41598-024-57659-x. Impact factor: 4.6

Viana, P., Hamar, P. (2024) Targeting the heat shock response induced by modulated electro-hyperthermia (mEHT) in cancer. Biochimica et Biophysica Acta (BBA) - Reviews on Cancer. 1879(2):189069. Doi: 10.1016/j.bbcan.2023.189069. Impact Factor: 11.2

Schvarcz, C.A., Danics, L., Krenács, T., **Viana, P**., Béres, R., Vancsik, T., Nagy, Á., Gyenesei, A., Kun, J., Fonovič, M., Vidmar, R., Benyó, Z., Kaucsár, T., Hamar, P. (2021) Modulated electro-hyperthermia induces a prominent local stress response and growth inhibition in mouse breast cancer isografts. Cancers (Basel). 13(7):1744. Doi: 10.3390/cancers13071744. Impact factor: 6.639

Publications not used in the dissertation

Aloss, K., Bokhari, S. M. Z., **Viana, P. H. L**., Giunashvili, N., Schvarcz, C. A., Szénási, G., Bócsi, D., Koós, Z., Storm, G., Miklós, Z., Benyó, Z., Hamar, P. (2024) Modulated Electro-Hyperthermia Accelerates Tumor Delivery and Improves Anticancer Activity of Doxorubicin Encapsulated in Lyso-

Thermosensitive Liposomes in 4T1-Tumor-Bearing Mice. Int. J. Mol. Sci. 25(6):3101. Doi: 10.3390/ijms25063101. Impact Factor: 5.6

Bokhari, S. M. Z., Aloss, K., **Viana, P. H. L**., Schvarcz, C. A., Besztercei, B. Giunashvili, N., Bócsi, D., Koós, Z., Balogh, A., Benyó, Z., Hamar, P. (2024) Digoxin-Mediated Inhibition of Potential Hypoxia-Related Angiogenic Repair in Modulated Electro-Hyperthermia (mEHT)-Treated Murine Triple-Negative Breast Cancer Model. ACS Pharmacol. Transl. Sci. 7(2):456–466. Doi: 10.1021/acsptsci.3c00296. Impact Factor: 6.0

Giunashvili, N., Thomas, J. M., Schvarcz, C. A., **Viana, P. H. L**., Aloss, K., Bokhari, S. M. Z., Koós, Z., Bócsi, D., Major, E., Balogh, A., Benyó, Z., Hamar, P. (2024) Enhancing therapeutic efficacy in triple-negative breast cancer and melanoma: synergistic effects of modulated electro-hyperthermia (mEHT) with NSAIDs especially COX-2 inhibition in in vivo models. Molecular Oncology. Doi: 10.1002/1878-0261.13585. Impact Factor: 6.6

Danics, L., Schvarcz, C.A., **Viana, P**., Vancsik, T., Krenács, T., Benyó, Z., Kaucsár, T., Hamar, P. (2020) Exhaustion of Protective Heat Shock Response Induces Significant Tumor Damage by Apoptosis after Modulated Electro-Hyperthermia Treatment of Triple Negative Breast Cancer Isografts in Mice. Cancers (Basel). 12(9):2581. Doi: 10.3390/cancers12092581. Impact factor: 6.639

10. Acknowledgements

I would like to start by expressing my deepest gratitude to God for His boundless blessings and strength throughout this journey. His unwavering presence provided me with the fortitude and inspiration needed to persevere in the face of challenges.

I am profoundly grateful to my supervisor Professor Péter Hamar for his guidance, support, and mentorship throughout the course of my research. His expertise and dedication played a pivotal role in shaping this thesis. I extend my sincere appreciation to Professor Zoltán Benyó for his support and for providing an environment conducive to academic growth. I truly felt like home working in the Institute of Translational Medicine. I am deeply grateful to my esteemed colleagues Dr. Csaba András Schvarcz, Dr. Lea Danics, and Dr. Tamás Vancsik for their warm welcome and invaluable assistance throughout my time here. Their profound expertise, particularly in mEHT, were essential for my experiments. Their willingness to share knowledge collaborate greatly to my research journey. I extend my thanks to my dedicated colleagues Balázs Besztercei, Zahra Bokhari, Kenan Aloss, and Nino Giunashvili for all their support and assistance throughout the experiments. Their collaborative spirit and technical expertise were pivotal in the successful execution of this research. I also would like to thank the lab assistants, Zoltán Koós and Dániel Bócsi, for their tireless administrative support, adept problem-solving, and dedicated efforts in handling paper submissions. I would like to thank to Oncotherm company for their generous provision of the Lab-EHY devices, as well as their dedicated maintenance and expert assistance. Their support played a crucial role in the successful execution of experiments and significantly contributed to the progress of this research. I would like to extend my gratitude to the entire Institute of Translational Medicine, both past and present colleagues, for their support, intellectual exchange, and collaborative spirit.

Finally, I am profoundly thankful for the unwavering support, love, and encouragement that my parents, sister, and entire family have demonstrated upon me, even from afar, throughout this academic journey. I miss you all!